TECHNISCHE UNIVERSITÄT WIEN

DIPLOMARBEIT

Computational Parametric Assessment of Microclimatic Heat Mitigation Measures in the Urban Domain

unter der Leitung von

Univ.-Prof. Dipl.-Ing. Dr. techn. Ardeshir Mahdavi

E 259/3 Abteilung für Bauphysik und Bauökologie

Institut für Architekturwissenschaften

eingereicht an der

Technischen Universität Wien

Fakultät für Architektur und Raumplanung

von

Karim Rezk, Bsc.

Matrikelnr. 01241927

[redacted]

Wien, September 2021

KURZFASSUNG

Die zunehmende sommerliche Überhitzung in Städten ist ein Indikator für das unangenehme städtische Mikroklima, dem Fußgänger im Sommer ausgesetzt sind und das auch den Kühlbedarf von Gebäuden erhöht. In dieser Arbeit wird die Effizienz verschiedener städtischer Strategien zur Eindämmung der Hitze während der Sommermonate in einem Untersuchungsgebiet untersucht, das aus vier großen Straßenschluchten besteht. Die wichtigste Maßnahme war die Erneuerung der versiegelten Asphaltflächen von Parkplätzen an den Straßenrändern durch unversiegelte Materialien. Ein weiterer Schritt war die Untersuchung der Auswirkungen der an den Außenfassaden der Gebäude vorgenommenen Änderungen auf das Mikroklima. In der Fallstudie machten die Parkplätze 8,5 % der simulierten Gesamtfläche aus. Die fünf angewandten Strategien, mit denen die asphaltierten Parkplätze und die Außenfassaden ersetzt wurden, sind: Rasengittersteine aus Beton, Vordächer zur Beschattung der Parkplätze mit Bepflanzung auf den Rasengittersteinen aus Beton, Fassaden mit hoher Albedo, grüne Fassaden an den massiven Außenhüllen der Gebäude und Bäume. Die Leistungsindikatoren der Studie sind Temperatur (°C), relative Luftfeuchtigkeit (%), Windgeschwindigkeit (m/s) und universeller thermischer Klimaindex (UTCI). Die Simulation wurde mit der Software ENVI-met durchgeführt, die die CFD-Methode verwendet, um die Ergebnisse für die genannten Indikatoren zu ermitteln, wobei jedoch der Faktor Regenwassertransport nicht berücksichtigt wird. Die Simulation für die fünf angewandten Strategien wurde für drei Fälle durchgeführt, zwei davon mit senkrechten Windrichtungen und der dritte mit einem symmetrischen Standortlayout, um die Rolle des Standortlayouts auf die Luftbewegung und ihre Auswirkungen auf die Mikroklimaindikatoren zu untersuchen. Bei den Temperaturergebnissen während der Tageshöchsttemperatur um 14.00 Uhr wurde der bemerkenswerte Temperaturrückgang durch begrünte Überdachungen und Bäume festgestellt. Bei den Ergebnissen für die Luftfeuchtigkeit um 14 Uhr wurde bei allen Strategien ein Anstieg des Verhältnisses der relativen Luftfeuchtigkeit aufgrund der angedeuteten Vegetation festgestellt. Die höchsten Werte für die relative Luftfeuchtigkeit wurden in den Szenarien mit Bäumen erreicht. Was die Windgeschwindigkeit betrifft, so haben nur grüne Baumkronen und Bäume eine bemerkenswerte Abnahme der Windgeschwindigkeit gezeigt. Der universelle thermische Klimaindex UTCI wird zur Bewertung des thermischen Komforts im Freien verwendet. Der bestehende Standort, das Beton-Gras-Gitter, die grünen Fassaden, die Fassaden mit hoher Albedo und die grünen Vordächer haben einen UTCI von über 32, was einer starken

Hitzestresszone entspricht. Das Szenario "Bäume" hat einen durchschnittlichen UTCI = 30,6, was in der moderaten Hitzestresszone liegt. Zur besseren Bewertung der Szenarien, bei denen die Gebäudefassaden verändert werden (grüne Fassaden und Fassaden mit hoher Albedo), wurde die Außenoberflächentemperatur einer einzelnen Zelle in der Mitte der Fassade eines Gebäudes am Standort berechnet. Die Ergebnisse zeigen, dass beide Strategien zwar einen bemerkenswerten Einfluss auf die Oberflächentemperatur und die Innentemperatur haben, aber nur einen minimalen Einfluss auf die Außentemperaturen haben. Die detaillierten Ergebnisse für jeden einzelnen Canyon zeigten, dass die Geometrie des Geländes in Bezug auf die Anordnung des Geländes, die Straßenbreite und die Gebäudehöhen in bestimmten Fällen einen größeren Einfluss auf das Mikroklima haben können als die angewandten Strategien im begrenzten Bereich von Parkplätzen oder den Außenfassaden. Zukünftige Forschungen sollten sich darauf konzentrieren, die Leistung der angewandten Strategien in anderen städtischen Gebieten mit unterschiedlichen Grundrissen und geometrischen Merkmalen zu vergleichen und den Regenwassertransport im Gelände zu berücksichtigen.

Stichwörter

Städtisches Mikroklima, Wärmeschutz, Thermische Behaglichkeit, Thermische Auswirkungen der Vegetation

ABSTRACT

Increasing summer overheating in cities is an indicator of the uncomfortable urban microclimate that pedestrians are subjected to during summer, which also increases the cooling demands of buildings. The thesis investigates the efficiency of different urban strategies for mitigating heat during summer period in a study area composed of four main urban canyons. The main measurement was to update the sealed asphalt surfaces of parking lots on the sides of the streets with unsealed materials. An additional step was exploring the impact of the changes applied to the external buildings' facades on the microclimate. In the case study, the parking lots formed 8.5% from the overall simulated area. The five applied strategies replacing the asphalt parking lots and the external facades are: concrete grass grid tiling, canopies to shade the parking lots with vegetation on the top added to the concrete grass tiling, high albedo buildings' blocks, green facades on the solid exterior buildings' walls and trees. The performance indicators of the study are temperature (°C), relative humidity (%), wind speed (m/s) and universal thermal climate index (UTCI). The simulation ran using ENVI-met software which uses CFD method to solve the results for the mentioned indicators, however it does not take rainwater transportation factor into account. The simulation for the five applied strategies ran for three versions, two of them with perpendicular wind directions and the third has a symmetrical site layout, in order to investigate the role of site layout on the air movement and its impact on microclimate indicators. In the temperature results during the peak temperature during day at 2pm, the notable decrease in temperature was recorded by vegetated canopies and trees. In humidity results at 2 pm, all strategies have recorded an increase in the relative humidity ratio due to the implied vegetation. The highest relative humidity values were reached in the trees' scenarios. In wind-speed results, only green canopies and trees have showed a remarkable decrease in the wind speed. The universal thermal climate index UTCI is used to evaluate the outdoor thermal comfort. The existing site, concrete-grass grid, green facades, high albedo facades and green canopies have UTCI higher than 32, which is a strong heat stress zone. Trees' scenario has an average UTCI = 30.6, which lie in the moderate heat stress zone. For a better evaluation of the scenarios where building facades are changed (green facades and high albedo facades), the outside surface temperature of a single cell in the middle of a façade of a building in the site was calculated. The results concluded that although both strategies have a remarkable impact on the surface temperature and the indoor temperature subsequently, they have a minimum effect on the outdoor temperatures. The detailed results for every single canyon showed that the site

geometry regarding site layout, street width and building heights can have in certain cases a higher influence on the microclimate than the applied strategies in the limited area of parking lots or the exterior facades. Future research should focus on comparing the performance of applied strategies in other urban areas with different layouts and geometrical characteristics and taking rainwater transportation in site into account.

Keywords

Urban Microclimate, Heat Mitigation, Thermal Comfort, Vegetation Thermal Impact

CONTENTS

1 INTRODUCTION

1.1 Motivation

In the recent years the number of heat days in Austria where temperature > 30°C is in constant increase (ADAPT-UHI, 2018). The discomfort resulted in the urban microclimate leads to a decrease of the time spent by city dwellers indoors, which increases the indoor energy consumption, decreases the contribution to economical and commercial activities and causes loss in the worker's productivity. Since 2005 50% of the population lives in cities (Brandenburg et al., 2018). Urban heat islands are urban areas experiencing higher temperature than surrounding areas. The dense layout of cities as well as sealed surfaces composed of asphalt and concrete contribute to the urban heat islands. The urban heat effect island risk index in Austria shows that 10% of Austria is subject to a degree of heat-related hazard where this includes main city centers. Population of urban areas consist of high percentage of vulnerable population categories (People aged 65 or older) compared to rural ones. Dense urban areas fall within high and very high hazard categories (Storch et al., 2020). Heat mitigation strategies and climate adaptation contribute to social cost-benefits through reducing hospitalization, mortality, and productivity loss. On the other hand, the ecosystem cost-benefits come up with reduction in stormwater runoff, reduce pollution and Co2 emissions, and decrease heating and cooling demands (ADAPT-UHI, 2018). Concerning outdoor thermal comfort there are three main factors: air temperature (Ta), relative humidity (RH), and wind velocity (WV). The hot and humid air gives the impression of suffocating and stale, causing breathing problems. The relative humidity of the air affects the amount of the heat discharged from the body during an evaporation. The intensity of an evaporation depends on the difference of partial pressure of water vapor on the surface of the skin and the water vapor contained in the air. The speed of an air movement affects the human's thermal sensation by disturbing the heat exchange by convection. Too high speed of an air flow creates a feeling of discomfort, cooling down the body (Dec et al., 2018). Vegetation can be immensely advantageous to heat mitigation through shading heat-absorbing surfaces and evapotranspiration cooling. However, the situation of each of urban canyons differs from one to another regarding the possibility of applying certain heat mitigation measurements. The situation is defined through the canyon's width, heights of buildings and functionality. Several studies have been conducted emphasizing the role of vegetation in heat mitigation in dense urban areas (Balany et al., 2020; Taleghani, 2018).

While new planning strategies for urban districts in recent domains employ simulations to assure the designs will meet a certain level of outdoor thermal comfort, existing cities lack possibilities of applying large scale solutions to mitigate urban heat and control the wind speed. Figure 1 shows the increase of number of days per year with temperature equal to or above 30°C from 1960 till 2018 in Mödling near Vienna. Figure 2 shows the map of urban heat vulnerability index (UHVI) in the dense urban fabric of Vienna, which illustrates the most sensitive and less resilient urban areas to extreme heat events.

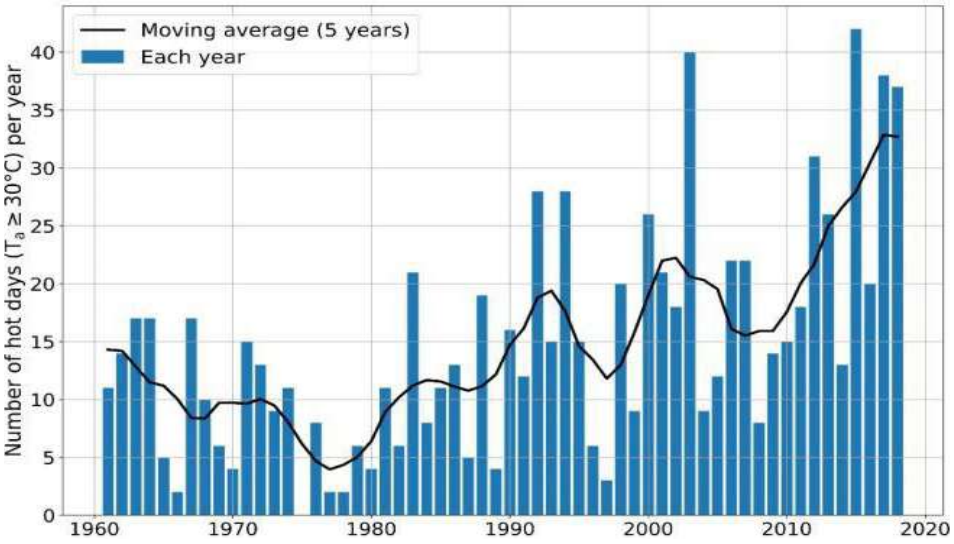

Figure 1. Number of hot days in Mödling from 1960 till 2018 (ADAPT-UHI, 2018)

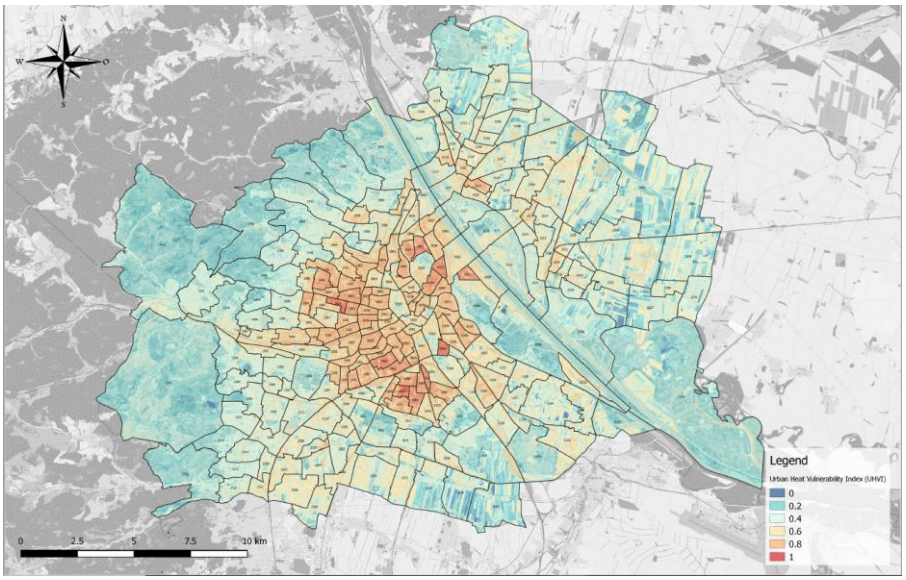

Figure 2. UHVI map of Vienna (ecoten, 2019)

The index is a composite of temperature data, data of green and blue infrastructure and demographic data. Transforming the functionality of whole urban districts to provide a vegetated area or banning traffic from certain streets to substitute the

impervious surfaces with porous ones is a rarely applied solution. The main challenge is to explore different scenarios to enhance the microclimate for the dense cities which are mainly planned in 18th and 19th centuries. In a dense urban canyon, the parking places are the simplest areas where a mitigation strategy can be applied as this will not block the traffic or apply changes to the existing structures. The research focused on replacing the asphalt materials of the parking lots on the street sides which range in width from 1.75m to 4m in the modeled site, applying greenery to all facades of the buildings and applying high albedo finishing material to the exterior walls and roof. The aim is to find out to which extent will every single strategy influence each of the performance indicators: temperature, relative humidity, wind speed and UTCI. The UTCI will provide an absolute evaluation of the outdoor thermal microclimate as in a single scenario the applied strategy can enhance one objective but at the same time disadvantage another one. The influence of the geometrical aspects in urban domain on the microclimate will be assessed, as the simulated site is modeled after an urban domain in the second district of Vienna, which consists of four main urban canyons with different orientations, widths and different shading caused by building structures of various heights. The width of the parking lots is directly proportional to the street width, which will question the feasibility of applying the microclimatic strategies in narrow streets on a small scale. The study implied five different strategies for the site model. Four of them are commonly used concepts: adding a bright reflective paint to the building blocks (AE), concrete-grass tiles in the parking lots (CG), green facades (GF), and trees (TR). The fifth one is using green canopies (GC), which are shading canopies with vegetation on top over unsealed ground surface. This strategy is inspired by the solution of Onishi et al., 2010 to mitigate UHI by greening parking lots. This strategy was tested due to the expected ability of shading, slowing wind-speed caused by their vertical structure, which are present characteristics in trees. Nevertheless, trees still need an expansion space in the depth of the ground layers, which can be impractical to apply in narrow urban canyons. Another objective to explore other cases than trees is that trees will make use of the parking lots, while other solutions will keep parking lots free for vehicles. Examples of the mentioned strategies are shown in Figure 3, Figure 4, Figure 5, Figure 6 and Figure 7.

Figure 3. High albedo blocks in Santorini (Marco Simoni)

Figure 4. Grass concrete tiling grid (wikiwand, 2007)

Figure 5. Green facade in Vienna (ADAPT-UHI, 2018)

Figure 6. Sketch of a green canopy parking lot (Onishi et al., 2010)

Figure 7. Photo of a street in Vienna shaded by trees (Matthias Winterer, 2019)

1.2 Research Questions

The current research aims to focus on the impact of microclimatic strategies on heat mitigation and outdoor thermal comfort using computational fluid dynamics (CFD) simulation of ENVI-met. The objective is to answer the following questions:

Q1. What is the influence of green strategies applied in the constrained areas of parking lots and facades on the microclimatic objectives: temperature, wind-speed, relative humidity, and thermal comfort level?

Results of the CFD simulation for the four proposed vegetation strategies, demonstrated through tables and graphs, will be compared to the conditions of a simulated existing site, and interpreted according to the assumptions made to decide which strategies to apply. Average results will be analyzed over twenty-four hours of simulation and detailed results for every urban canyon will be explored at 2pm.

Q2. How strong is the influence of the urban domain's geometrical attributes on the microclimate?

The geometrical attributes of the site ranging from the street network, streets orientation and building heights influence the shading and wind direction. Results of urban canyons with same orientation but different width or buildings' heights will be thoroughly investigated. Another step taken is to run three simulations for each of the existing site model and the five applied scenarios, where the first simulation uses a wind direction = 150°, second simulation uses wind direction = 60°, third simulation uses wind direction = 150° but with an added building at the intersection of two main streets to add symmetry to the site layout.

Q3. How can the results of the applied numerical simulation tool (ENVI-met) be evaluated?

ENVI-met is a software that can simulate climates in urban environments and assess the effects of atmosphere, vegetation, architecture, and materials. ENVI-met doesn't support water flow in site, no turbulent mixing is included in the model so that the use is restricted to still waters (e.g., lakes). It is crucial to mention that the simulation takes place on August 2nd, where in August number of rain days = 8.5 as shown in Figure 8. So, the simulation model will not take into consideration the absorption and storage of moisture in urban environment. Permeable pavements contain more air voids than conventional impermeable pavements and they are designed to allow water to drain into the sublayers and then down into the groundwater. Permeable pavements have many environmental advantages compared to conventional pavements, including reducing stormwater run-off, recharging of groundwater, reducing the discharge of

pollutants, improving air quality, and reducing noise on roads and highways (Ferguson, 2005; Scholz & Grabowiecki, 2007). Besides these benefits, their relatively high porosity allows permeable pavements to store water when wet. This water can be made available for evaporation during hot times of the day, thus reducing surface and air-temperatures through evaporative cooling (Li et al., 2013). Consequently, evaluating the replaced asphalt with concrete grass tiling grid or soil for trees' planting will depend on the albedo values and evapotranspiration of the greenery.

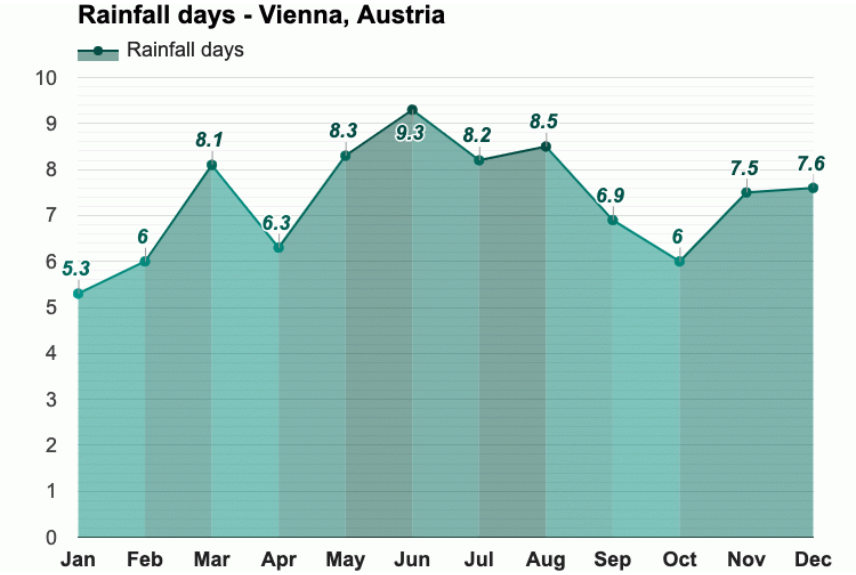

Figure 8. Rainfall days in Vienna (Zentralanstalt für Meteorologie und Geodynamik, 2021)

1.3 Background

1.3.1 Overview

Previous studies have considered thoroughly the effect of vegetation and exchanging sealed surfaces with unsealed ones on urban microclimate. Dimitrova et al., 2014 have published a study investigating the capabilities of vegetation and albedo values of surfaces to attenuate microclimatic extremes by combining on-site measurements and numerical simulations for several scenarios applied to two parallel canyons similar in orientation and geometry. The higher surfaces' albedo and addition of trees will achieve a high reduction of summer extreme temperatures.

Aleksandrowicz et al., 2017 analyzed the research trends in urban heat island mitigation, which are mainly shade trees, cool building envelopes, ground vegetation and green roofs. It is concluded that the more studied mitigation measurements are those which can be easily implied in dense urban fabrics. Therefore, street geometry had a less attention in the research compared to other mentioned research trends.

According to Lim et al., 2014, metropolitan areas worldwide display highly diverse microclimatic conditions that are believed to be influenced by a variety of parameters: morphologies, structures, materials (particularly urban surface properties), and processes (mobility, industry, etc.). The density of urban structures and sealing of urban areas may lead to higher heat storage, thus increasing the daily urban air temperatures.

The review paper presented by Nasrollahi et al., 2020 was exploring the impact of various strategies on pedestrian thermal comfort. The review covered both field work and simulations. Results found out that between water bodies, solar reflective materials, vegetation, and geometry of urban forms vegetation and specifically trees due to their shading effect. Also, the ratio of height to width (H/W) in urban canyons is directly proportional to the thermal comfort.

Ferrari et al., 2020 have investigated the impact of reflective and permeable surfaces on the microclimate. The approach yielded detailed analysis for the impact of pavements and meteorological conditions (wind, sun, rain) on the storage and absorption of heat and moisture in urban environments. The study was conducted for a single canyon with a single rain event. After a rain event, composite materials with higher reflectivity and porosity showed high cooling effect compared to dark dense ones.

Djedjig et al., 2017 have conducted an experimental study of vegetated facades and their hygrothermal effects. The results of outdoor analysis showed that the green wall tested reduced until 1.5 °C of the temperature rise within the canyon.

1.3.2 Thermal Comfort

Thermal comfort can be described as following:

> „Thermal comfort is the condition of mind that expresses satisfaction with the thermal environment and is assessed by subjective evaluation“ *(Ashrae, 2017, p. 3).*

The six factors affecting thermal comfort are both environmental and personal. These factors may be independent of each other, but together contribute to a human's thermal comfort. Environmental factors: air temperature, radiant temperature, air velocity and humidity. Personal factors are clothing insulation and metabolic rate.

Universal thermal climate index UTCI

UTCI was developed in 2009 by virtue of international co-operation between leading experts in the areas of human thermophysiology, physiological modelling, meteorology, and climatology (Błażejczyk et al., 2013). UTCI is the equivalent temperature for the environment derived from a reference environment. It is defined as the air temperature of the reference environment which produces the same strain index value in comparison with the reference individual's response to the real environment. It is regarded as one of the most comprehensive indices for calculating heat stress in outdoor spaces. This index was developed to have a standard criterion for assessing heat stress in the light of human meteorology (Błażejczyk et al., 2010). The input data for calculating UTCI include meteorological and non-meteorological (metabolic rate and clothing thermal resistance) data (Farajzadeh et al., 2016). The parameters that are considered for calculating UTCI involve dry temperature, mean radiation temperature, the pressure of water vapor or relative humidity, and wind speed (at the elevation of 10 m). Figure 9 reveals the procedure.

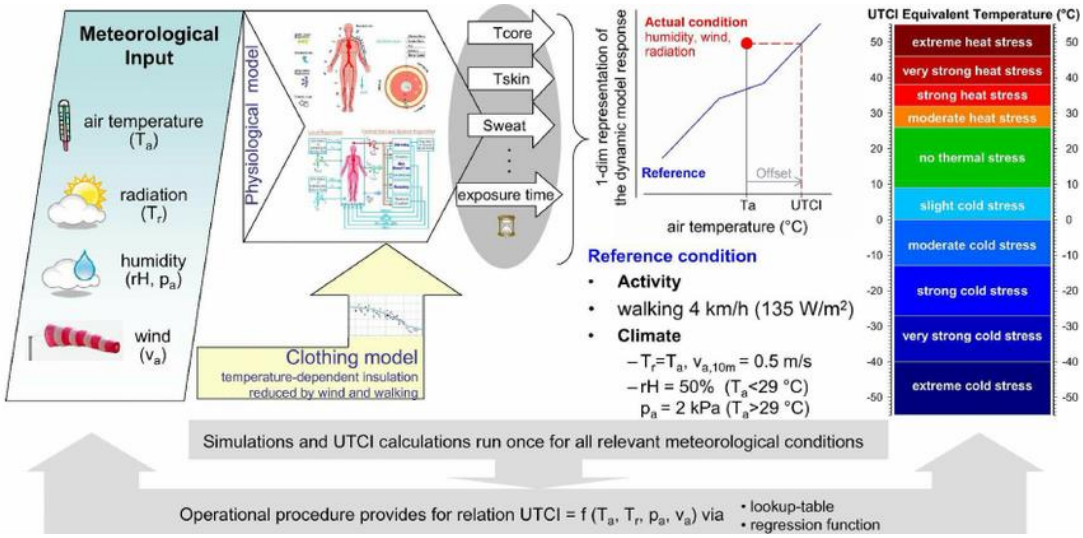

Figure 9. Elements of the operational procedure and concept of UTCI as categorized equivalent temperature derived from the dynamic response of a thermo-physiological model coupled with a behavioural clothing model (Błażejczyk et al., 2013)

UTCI is divided into 10 groups ranging from extreme cold stress to extreme heat stress (Young, 2017) as shown in Figure 10. The wind speed should range from 0.5 to 17 m/s in order to calculate UTCI (Fröhlich & Matzarakis, 2015). UTCI is defined as the air temperature (Ta) of the reference condition causing the same model response as actual conditions. The offset, i.e., the deviation of UTCI from air temperature, depends on the actual values of air and mean radiant temperature (Tmrt), wind speed (va) and humidity, expressed as water vapour pressure (vp) or relative humidity (RH). This may be written in mathematical terms as:

$$UTCI = f(Ta; Tmrt; va; vp) = \\ = Ta + \text{Offset}(Ta; Tmrt; va; vp) \quad (1)$$

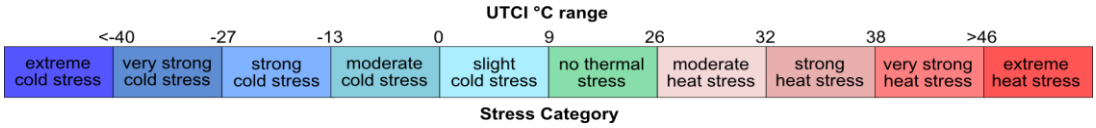

Figure 10. UTCI range (Climate Chip, 2021)

2 METHOD

2.1 Simulation Workflow

The workflow of the simulation process as represented in Figure 11 started by modeling the geometry of the study area in Rhinoceros. The model was linked to Grasshopper internalized software in Rhinoceros, where the data of EPW weather file was imported and the geometry was converted to Envi-met 2mx2mx2m grid model using Dragonfly plug-in in Grasshopper which contains an Envi-met extension developed by Antonello Di Nunzio. The asphalt surfaces of vehicle transport were assigned as constant material, while the parametrized surface materials for parking lots on the sides of the streets and building facades were grouped together and each single strategy was selected depending on each scenario. By selecting the scenario an “INX” ENVI-met model and “simx” ENVI-met simulation file are exported directly. The model and simulation files are copied to the cloud computing virtual machine and the simulations ran on the server.

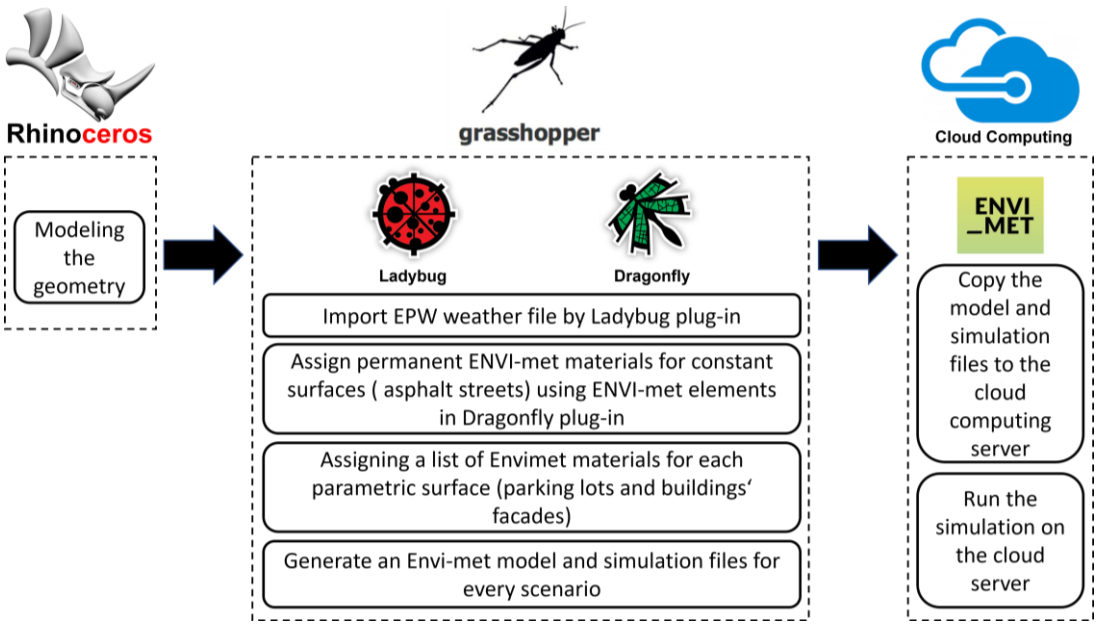

Figure 11. Workflow of the simulation process

2.2 Study Area

The site of the CFD study is modeled after an urban quarter of area = 150m x 200m in the second district of Vienna displayed in Figure 12. The Four main streets: Große Stadtgutgasse, Glockengasse, Pillersdorfgasse and Novaragasse are modeled as Street_1, Street_2, Street_3, Street_4 respectively as shown in Figure 13.

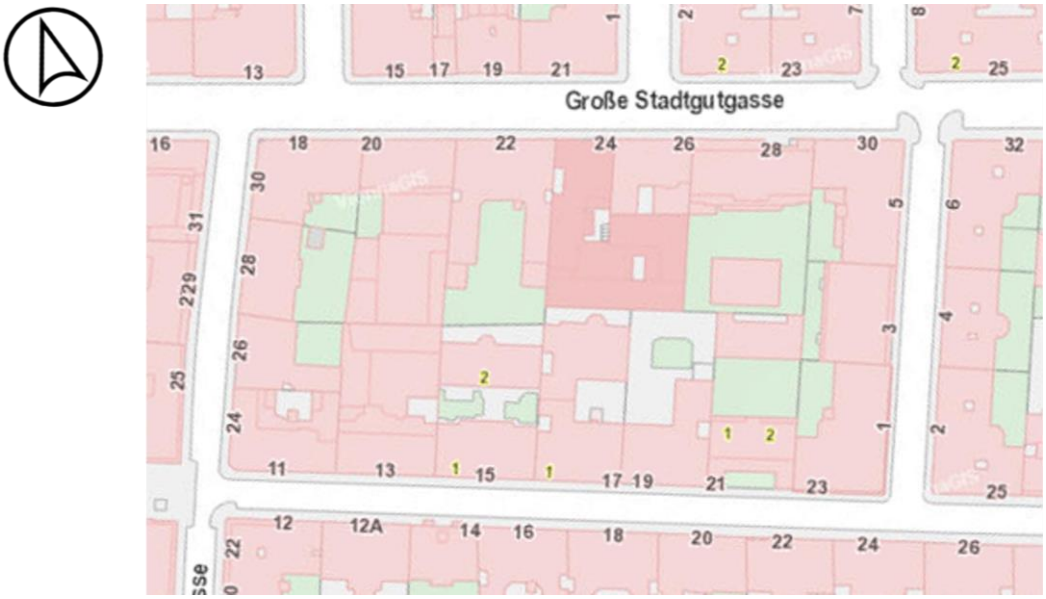

Figure 12. Map of the study area (Stadt Wien, 2021)

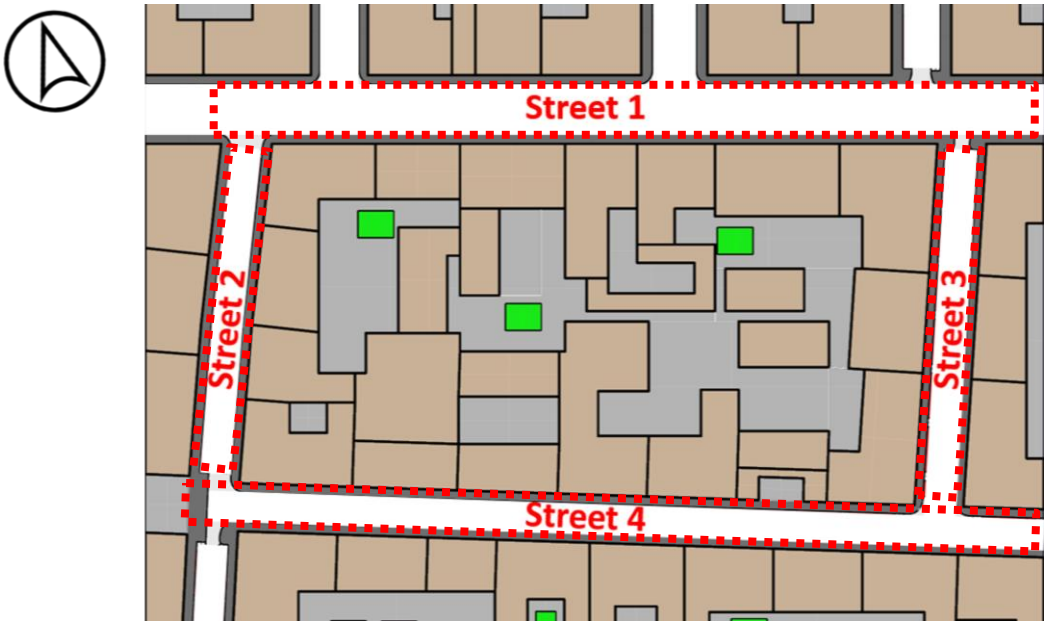

Figure 13. Street_1, Street_2, Street_3 and Street_4 with their boundaries in site

Street_2, Street_3 and Street_4 have no branching streets. Street_1 has 3 branching streets in north-north-east direction (NNE). The average heights of buildings in the four streets = 21m. Table 1 shows the width of each street. The sections of the site are illustrated in Figure 14 and Figure 15.

Table 1. Width of each urban canyon

	Street_1	Street_2	Street_3	Street_4
Width	15.3	11.3	10.9	10.7

Figure 14. Section through Street_1 and Street_4

Figure 15. Section through Street_2 and Street_3

Site Modelling

The site was modeled in Rhinoceros after the downloaded map from city plan section in city of Vienna official website in “PDF” format. The ENVI-met model doesn’t create solid surfaces or volumes with slopes, instead it remodels these elements from rhinoceros into 3D grid-based elements. The existing site scenario contained buildings with default ENVI-met moderate wall insulation material and terracotta roofing. The two modeling phases are shown in Figure 16.

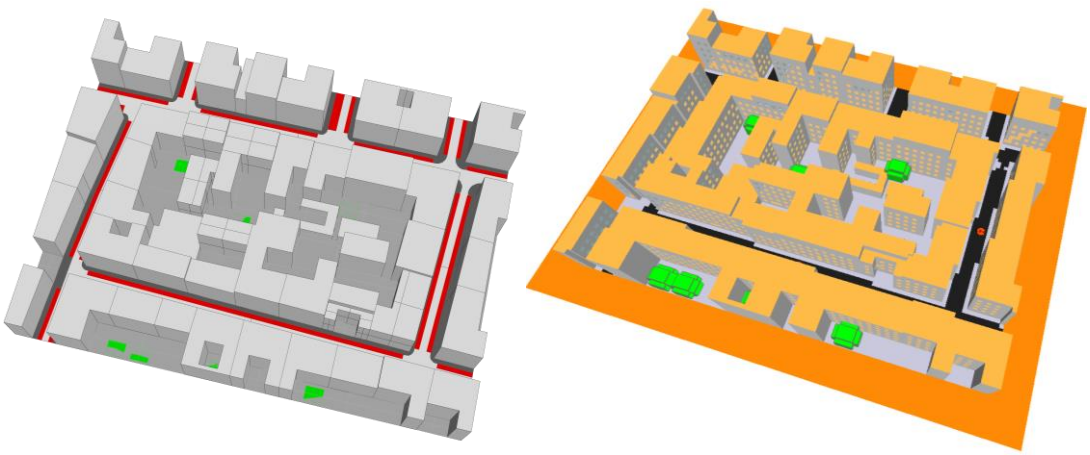

Figure 16. Rhinoceros model on the left and ENVI-met model on the right

2.3 Assessed Scenarios

The following five assessed strategies are applied to the existing site model in three versions. Version A has a prevailing wind direction = 150 °, version B has a prevailing wind direction = 60 ° and version C has the same wind direction as version A but it includes an extra building block at the intersection of Street_2 and Street_4. The strategies and their versions resulted in the totally 18 scenarios, as shown in Table 2.

Table 2. Scenarios and their nomenclature

	Wind direction (see Chapter 2.7.1)		
	150° (A)	60° (B)	150° (C)
	Site layout		
	Asymmetrical (A)	Asymmetrical (B)	Symmetrical (C)
Existing site	EX_A	EX_B	EX_C
High albedo blocks	AE_A	AE_B	AE_C
Concrete-grass tiling	CG_A	CG_B	CG_C
Green facades	GF_A	GF_B	GF_C
Green canopies	GC_A	GC_B	GC_C
Trees	TR_A	TR_B	TR_C

2.3.1 Strategies and their modeling elements

2.3.1.1. High Albedo blocks (AE) model

All the building envelopes of the building site are coated by a high albedo reflective material. This includes the exterior walls on the sides of the streets, the exterior walls in courtyards and the roofs of the buildings.

The high albedo blocks' scenario (AE) as shown in Figure 17 applies a bright paint material to the facades and roofs of the buildings with an RGB-value = (230, 230,230), while the walls of buildings in existing site model had an RGB-value = (128,128,128) and the terracotta roofing in existing site model had an RGB-value = (193,133,51).

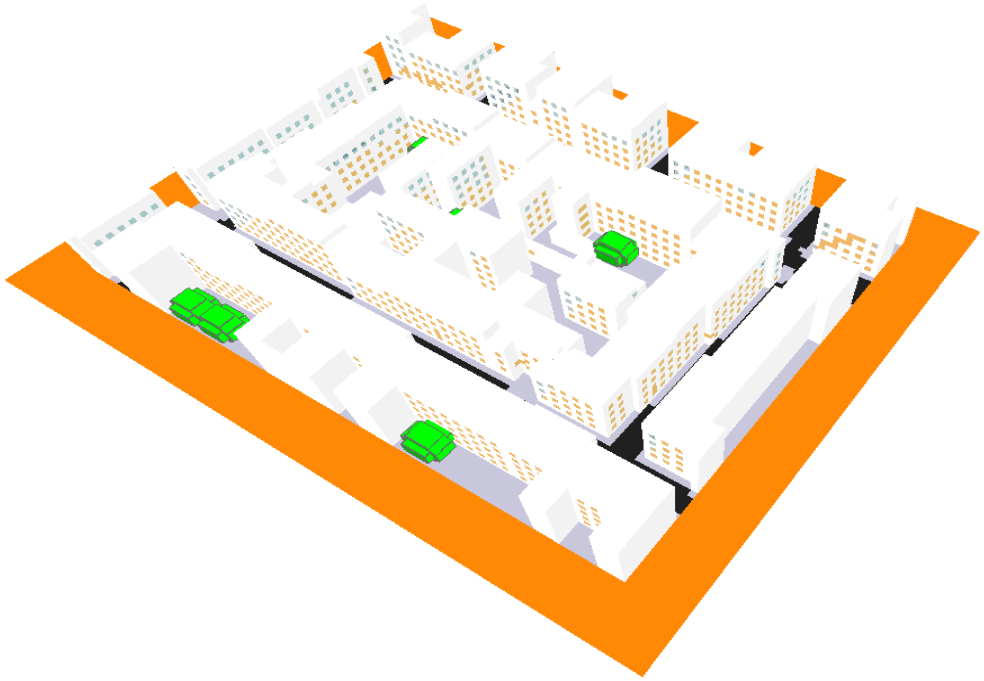

Figure 17. High albedo blocks' strategy

2.3.1.2. Concrete-grass tiling (CG) model

The asphalt surfaces of the parking lots will be changed by permeable concrete-grass tiling.

As the Envi-met software offers a maximum detail = 0.5 x 0.5m, modeling tiny, detailed concrete grass (CG) grid tiling was impossible, considering that the resolution level applied in simulations = 2 x 2m. According to the consultation of Envi-met developers, the solution was to model a grass component in the Envi-met plant data manager with the average albedo value equal to the average albedo values of grass and concrete = 0.3 and the grass root depth was minimized to 0.2 instead of 0.5. Figure 18 shows the resulted site model with concrete-grass tiling grid.

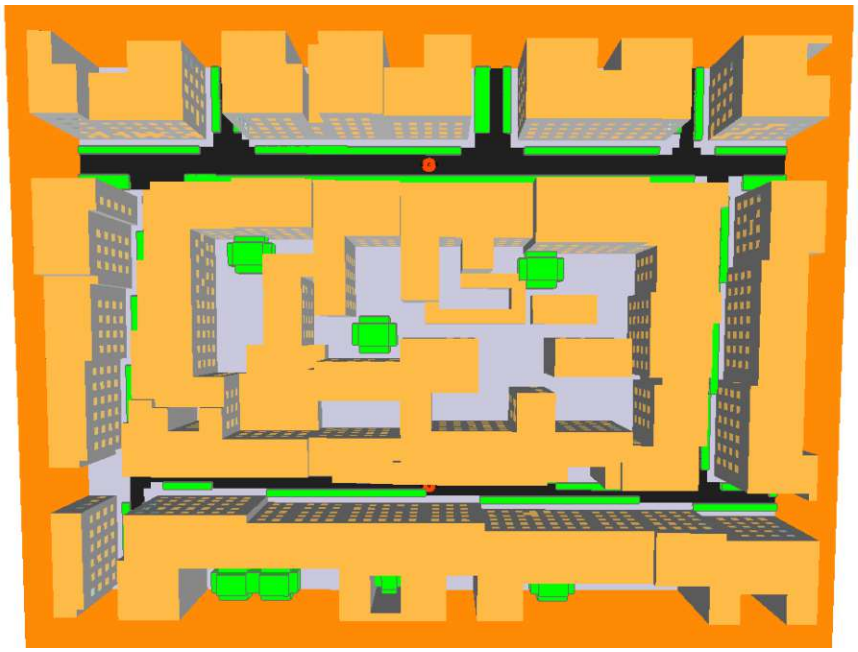

Figure 18. Concrete grass tiling strategy

2.3.1.3. Green facades (GF) model

The greening is applied to all external walls of the buildings, including the exterior walls in the inner courtyards. The green walls are not depending on the vertical framework structures supporting the branch system of the plant, instead the greening is applied on a substrate layer of sandy loam and Styrofoam followed by an air gap layer separating it from the wall of the building.

Vegetated walls can be simulated in Envi-met to include the effects of different growing mediums and mounting methods for the plants. The default façade greening in the ENVI-met database with air gap = 0.1 and mixed substrate was applied. The green facades' Envi-met model is shown in Figure 19.

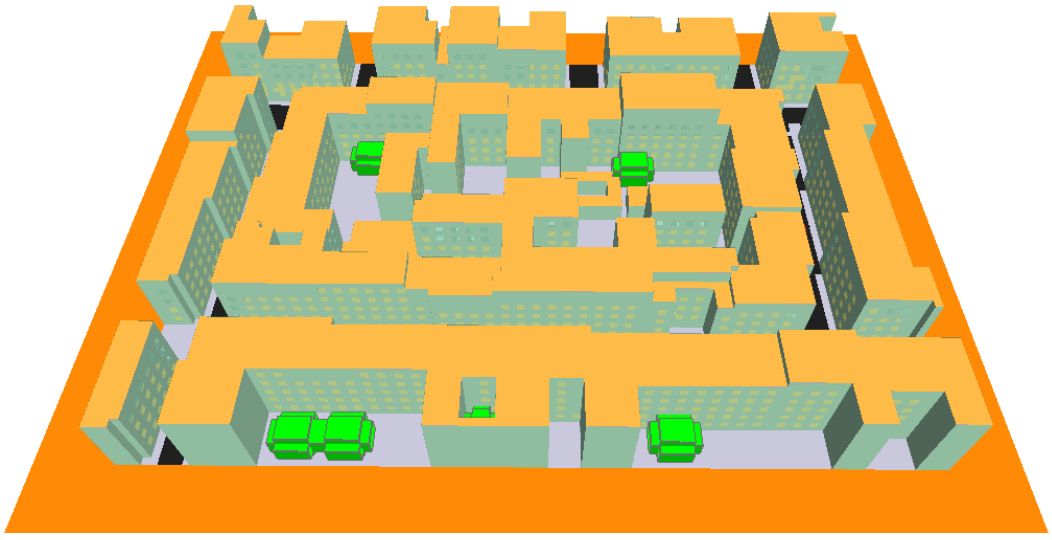

Figure 19. Green facades' strategy

2.3.1.4. Green canopies (GC) model

The concept of the green canopies depends on adding an extra sun sail transmissive canopy with vegetation on the top to parking lots with concrete-grass tiling.

The canopies consist of two elements, the solid structure of the canopy was modeled as horizontal planes assigned the sun sail material from single wall category in the Envi-met database and the vegetation part was modeled as plant from hedges group added to the database with height = 2.4m and a RAD-profile divided to ten equal parts, nine of them had RAD = zero and the tenth upper part had a RAD = 3. Figure 20 represents a street in the site model with green canopies.

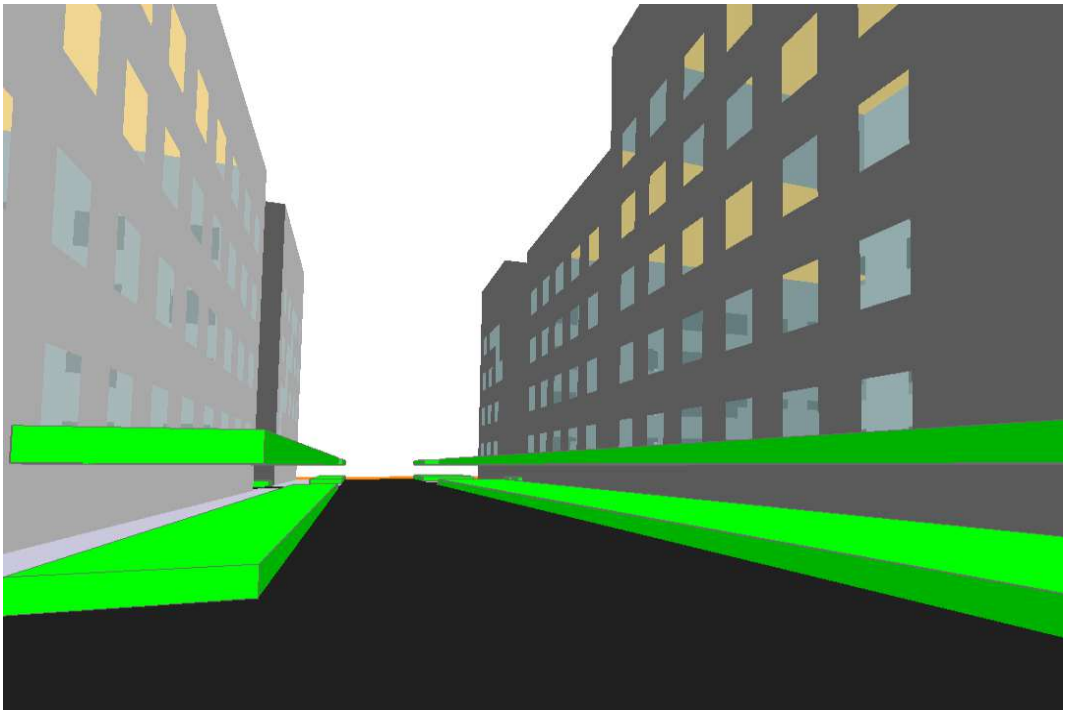

Figure 20. Green canopies strategy with concrete grass tiling

2.3.1.5. Trees (TR) model

The trees scenario applies planting trees in all the spaces of parking lots.

Trees were a critical component to model, as the tree height, root area width and root depth should be convenient to the street width. A customized tree was modeled in the Albero plug-in released by Envi-met as shown in Figure 21 with the following properties: trunk: medium size, height = 8m, width = 4m, LAD-profile: high, form: cylinder, root depth = 4.8m and root diameter= 4.8m. The proposed tree parameters were derived from the online trees and green spaces database of Vienna city “Wien Umweltgut” (Stadt Wien-MA 42, 2021), where the crown diameter of planted trees in similar streets to the model was ranging from 4-6m and height was ranging from 6-10m.

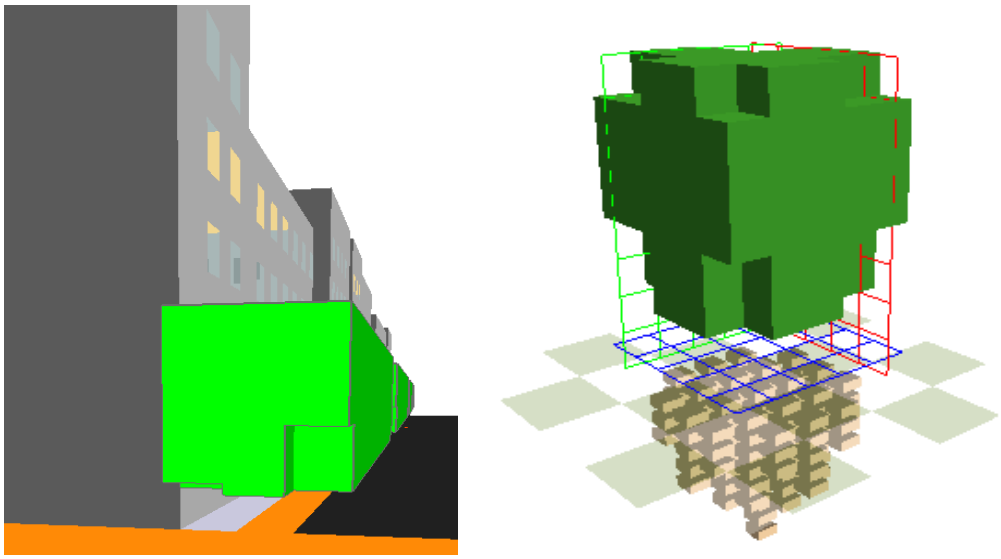

Figure 21.Trees in the ENVI-met model on the left and tree modelling in Albero on the right

2.3.2 Simulation versions

Each of the six applied strategies is simulated in three versions, resulting in a total number of eighteen scenarios. First version (version A) has a wind direction = 150°. While second version (version B) has a wind direction = 60°. Third version (version C) has a wind direction = 150° with an extra building block at the intersection of street_2 and street_4. Figure 22, Figure 23 and Figure 24 represent the three versions.

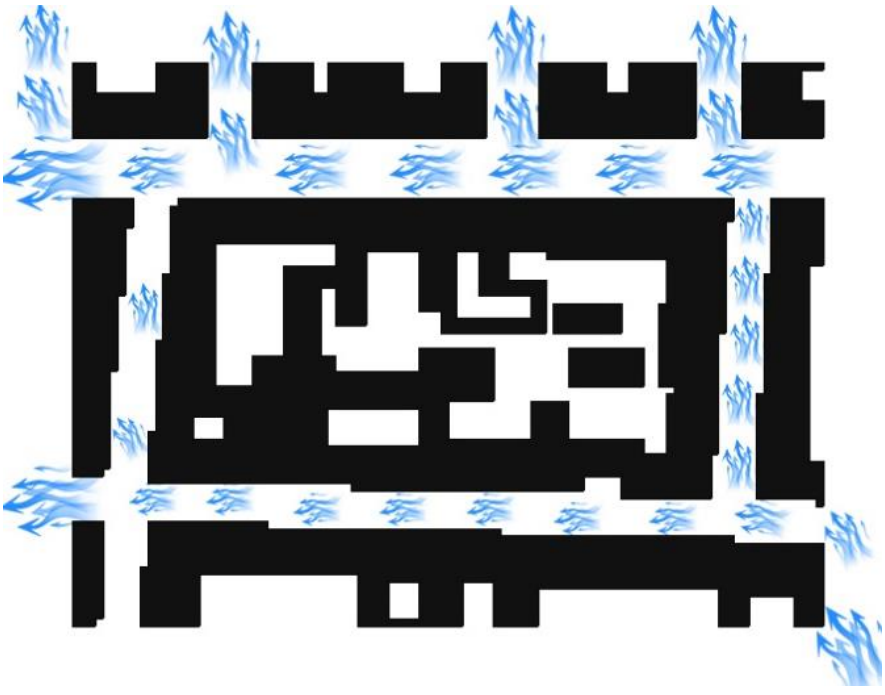

Figure 22. Version A, wind direction = 150°

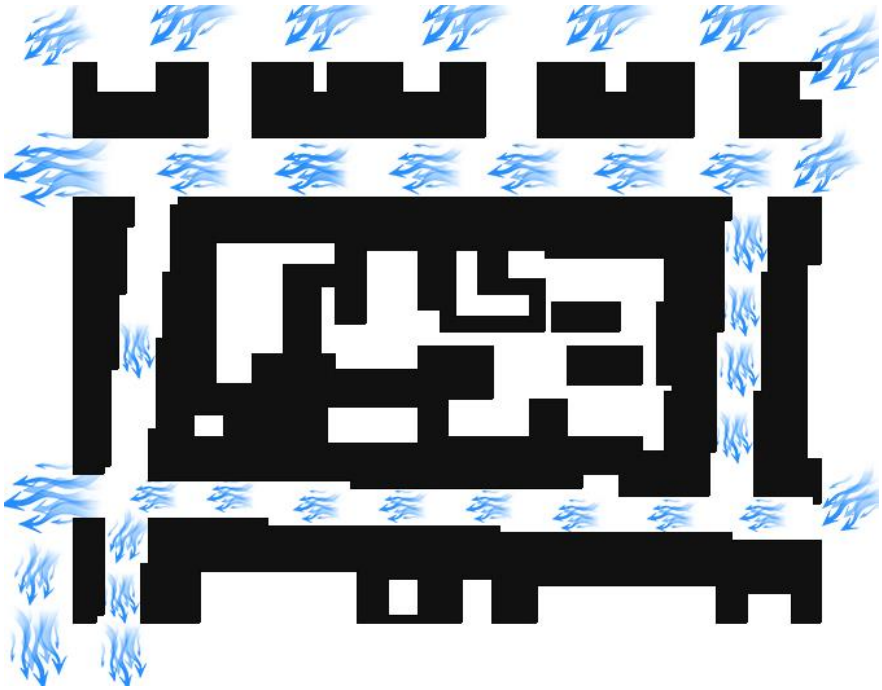

Figure 23. Version B, wind direction = 90°

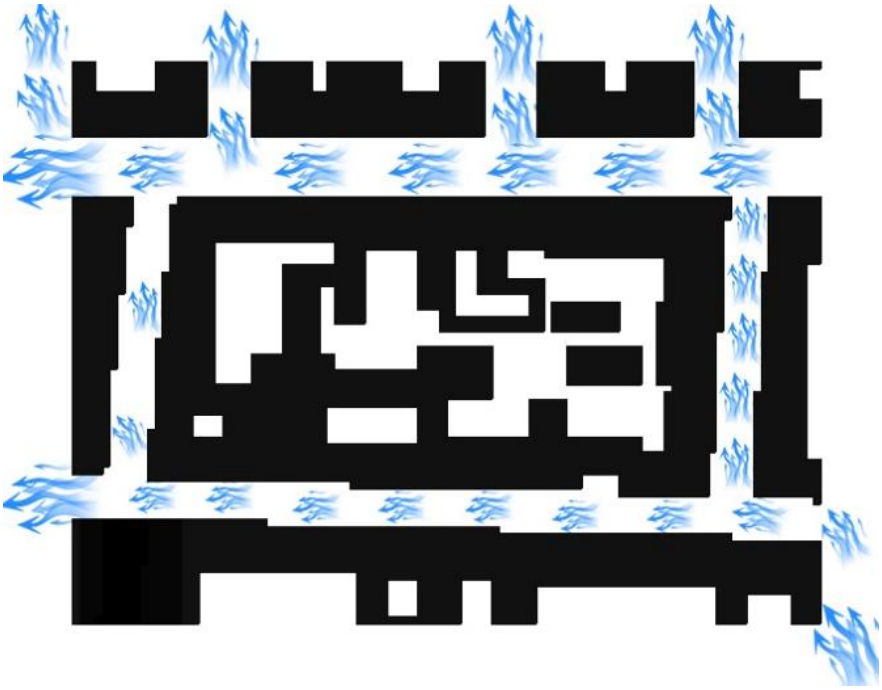

Figure 24. Version C, symmetrical layout with wind direction = 150°

2.4 Weather file and Boundary Conditions

The weather file was extracted from energy plus online weather data for Vienna Schwechat 110360 in ".epw" format. The extracted data from weather files as boundary conditions for the simulation were on 1st of August at 2 pm.

The temperature, relative humidity, wind-speed were imported from the "EPW" Vienna weather file directly, only the wind-direction varied in the second version B. Table 2 shows the values of the initial boundary conditions on 1st of August at 2 pm.

Table 3. initial boundary conditions

Temperature (°C)	30
Relative Humidity (%)	34
Wind Speed (m/s)	5
Wind direction (version A)	150
Wind direction (version B)	60

2.5 Statistical Analysis

The Envi-met exports atmosphere data for every hour in an output file. The Leonardo plug-in has accessed the atmosphere data generated by ENVI-met simulation. Through Leonardo atmospheric temperature maps with wind flow were extracted as well as CSV tables of grid cells for temperature, relative humidity, and wind-speed at Z-axis (height) = 1.4 m. The grid cells of the four main streets were selected in Excel from the whole site grid for further analysis.

3 RESULTS

3.1 Overview

This chapter presents the results of simulations for the eighteen different scenarios in version A, version B and version C. The simulation results for 24 hours will be discussed on the level of the average results of the four main streets. The last simulation result at 2 pm on the third of August (next day of simulation) are the most accredited results as the shift of the ENVI-met results from the boundary conditions is directly proportional to the duration of simulation. Therefore, the results at 2 pm on the average results for each single street from Street_1, Street_2, Street_3 and Street 4 will be discussed. This deeper exploration will give a more accurate explanations for the results according to the geometrical and climatic factors of elements in the site.

3.2 Graphs of aggregated results for the whole study area

In the graphs section, the average results of temperature, humidity, and wind speed for Street_1, Street_2, Street_3 and Street_4 in the 6 simulated strategies: existing site (EX), high albedo blocks (AE), concrete grass tiling grid (CG), green facades (GF), green canopies (GC) and trees (TR) in version A, version B and version C are plotted for 24 hours in 2D-line type chart. Average temperature results are shown in Figure 25. Average relative humidity results are shown in Figure 26. Average wind speed results are shown in Figure 27.

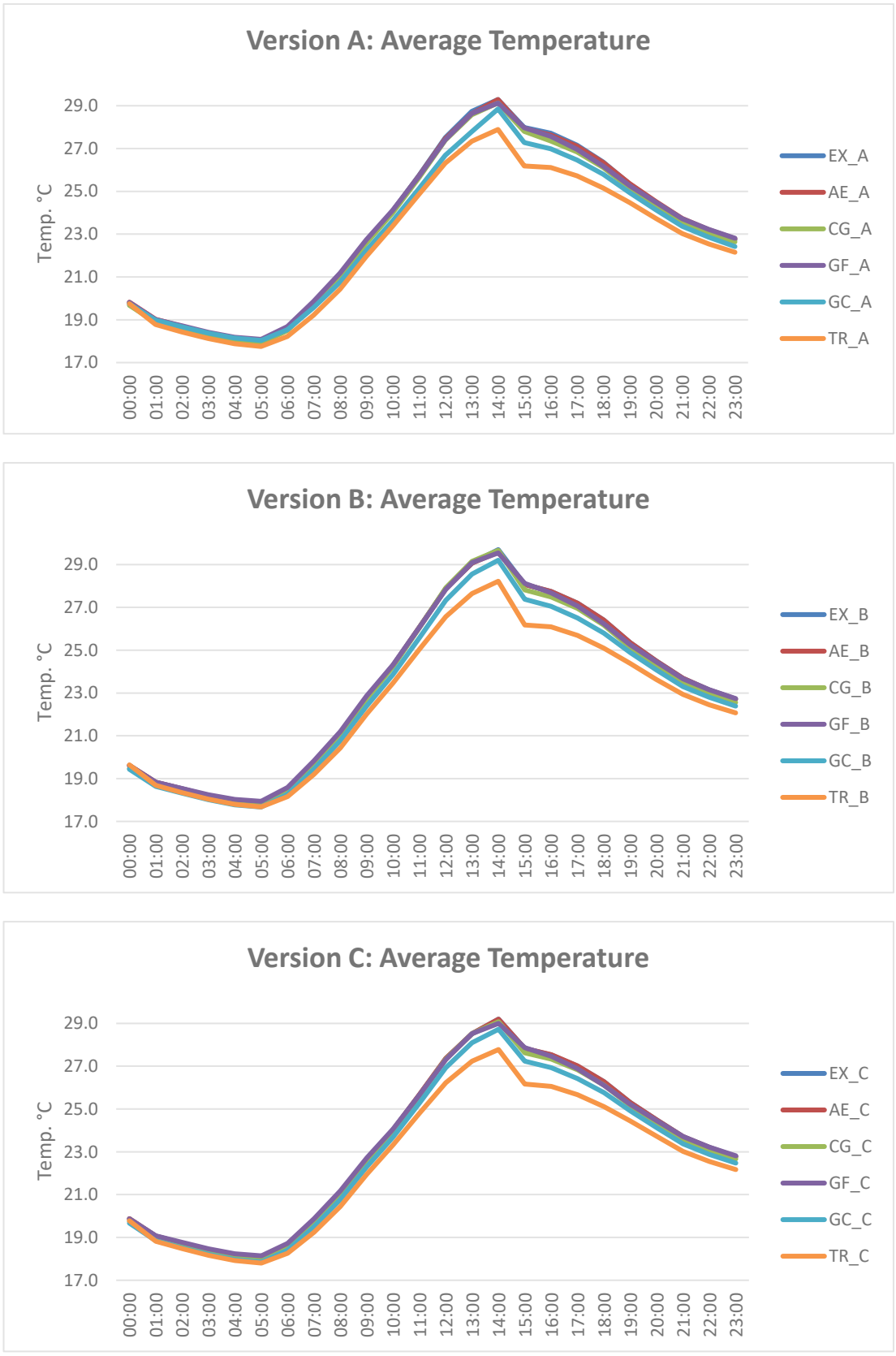

Figure 25.Average temperature values for version A, version B and version C

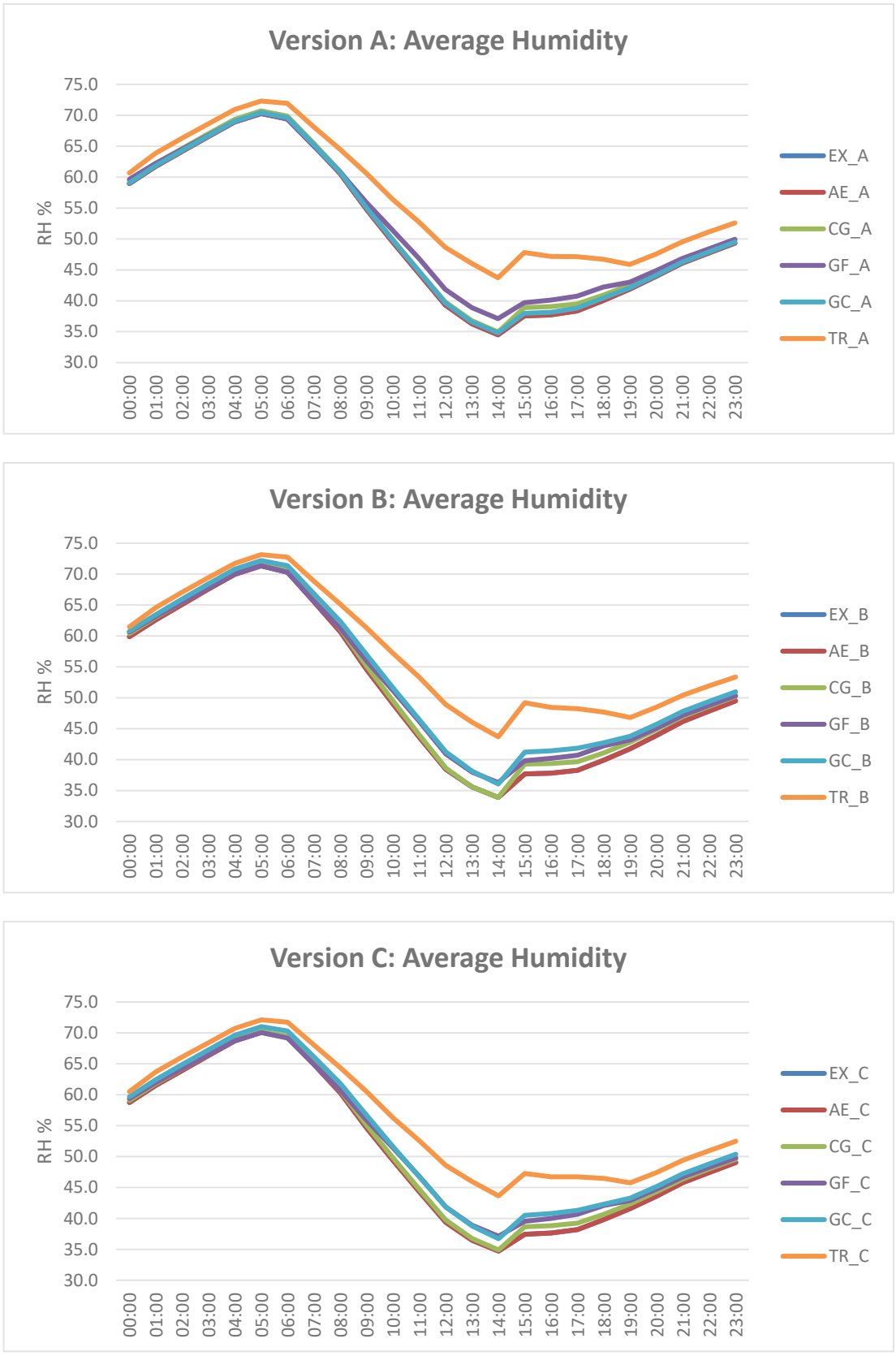

Figure 26.Average Humidity values for version A, version B and version C

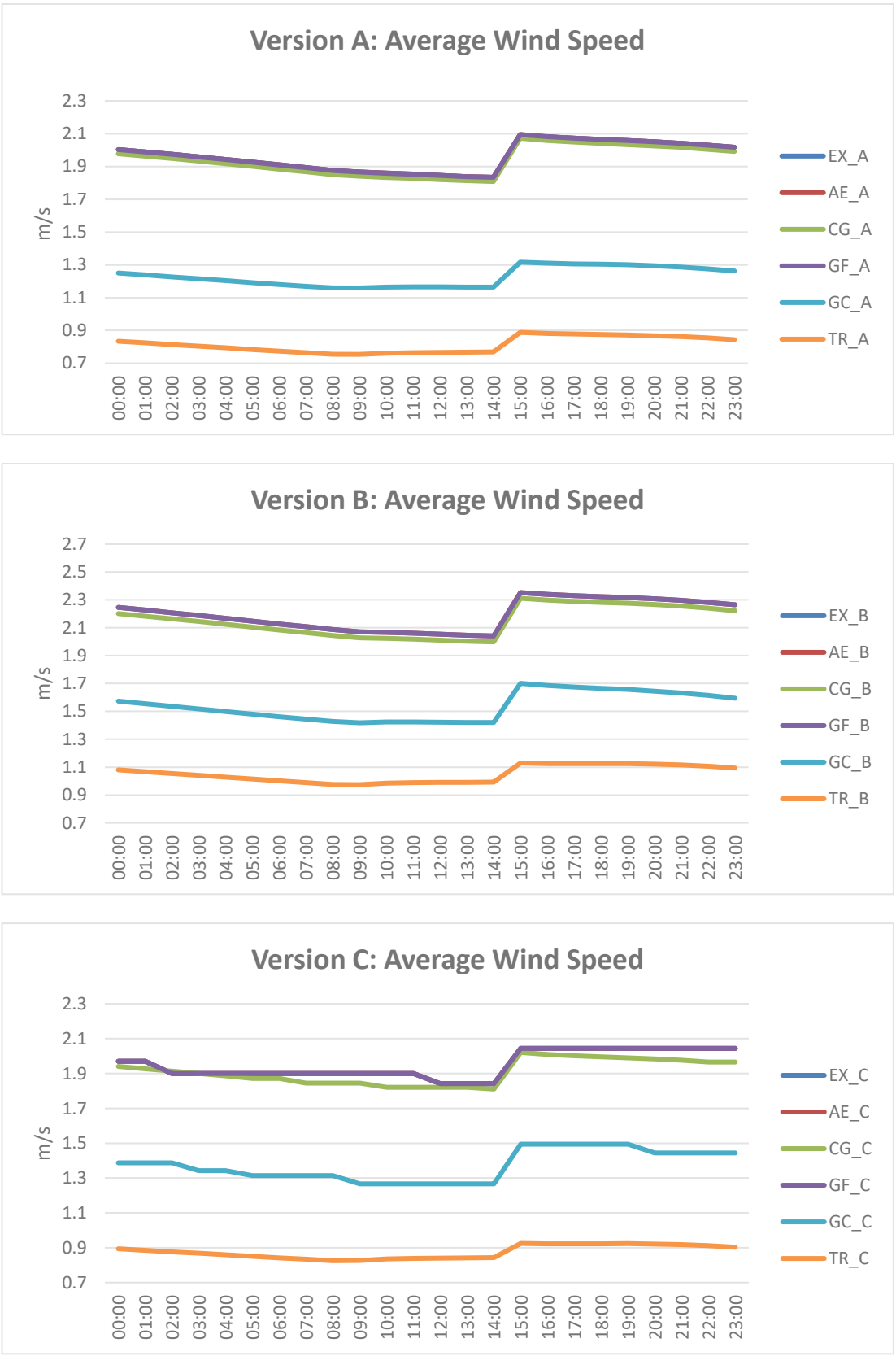

Figure 27. Average wind speed for version A, version B and version C

3.3 2D maps from ENVI-met

The 2D generated color maps for the 18 scenarios in version A, version B and version C at 2 pm illustrate the air temperature at height = 1.4m and the air flow direction in different urban canyons. The maps are exported from Leonardo plug-in. Every map has maximum temperature, minimum temperature and a legend explaining temperature ranges represented by different colors. The maps for scenarios with version A are shown in Figure 28, Figure 29, Figure 30, Figure 31, Figure 32, and Figure 33. The maps for scenarios with version B are shown in Figure 34, Figure 35, Figure 36, Figure 37, Figure 38 and Figure 39. The maps for scenarios with version C are shown in Figure 40, Figure 41, Figure 42, Figure 43, Figure 44, and Figure 45.

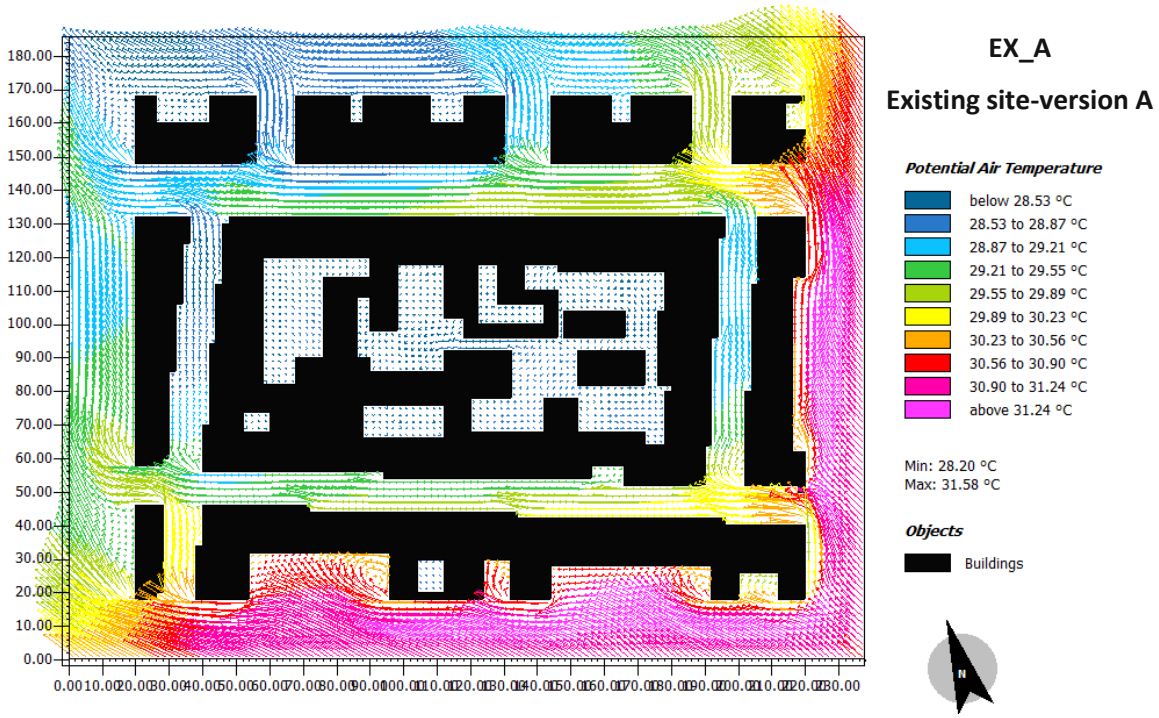

Figure 28. 2D map of EX_A

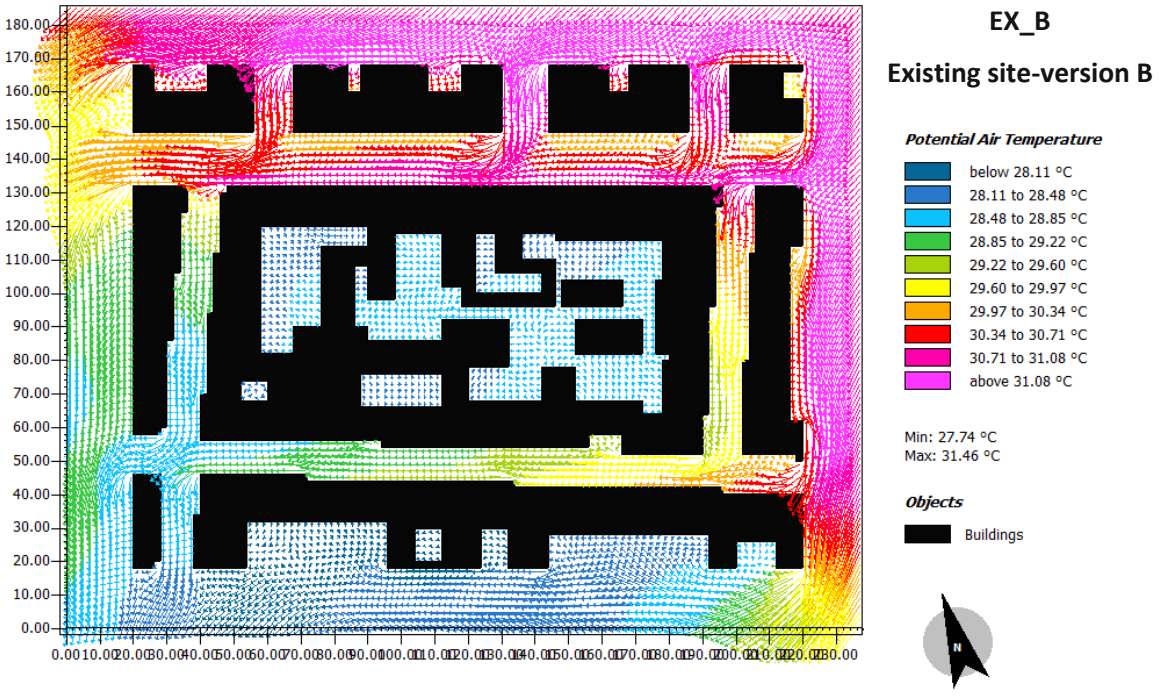

Figure 29. 2D map of EX_B

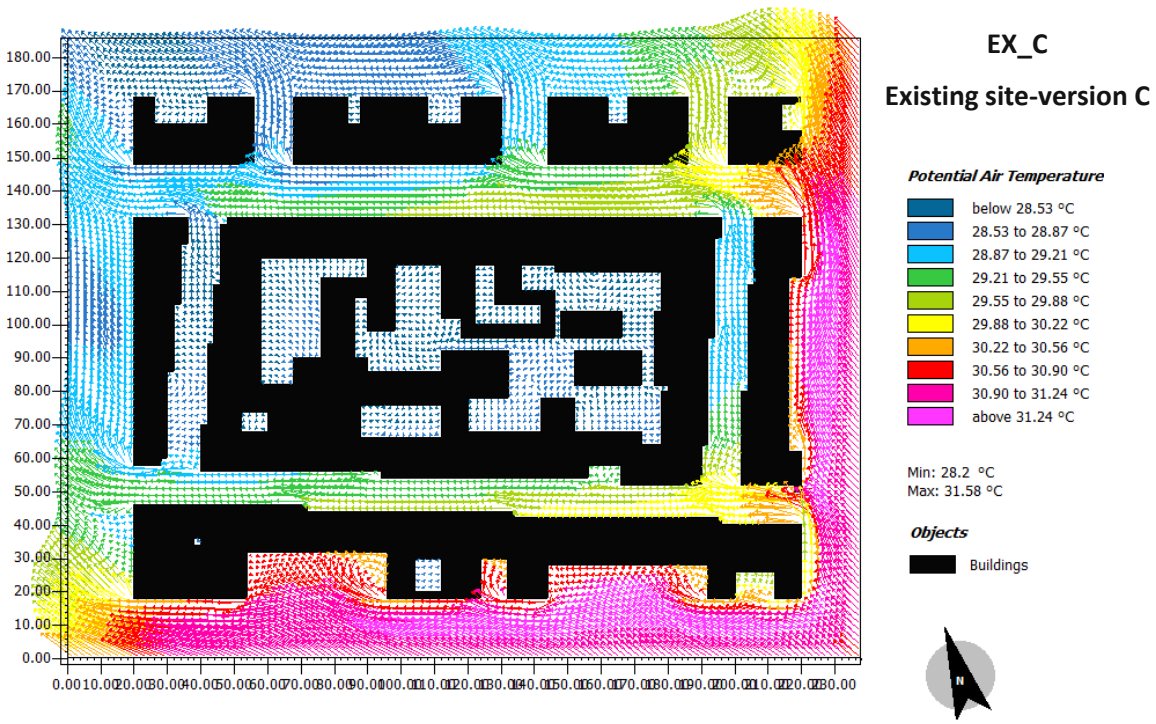

Figure 30. 2D map of EX_C

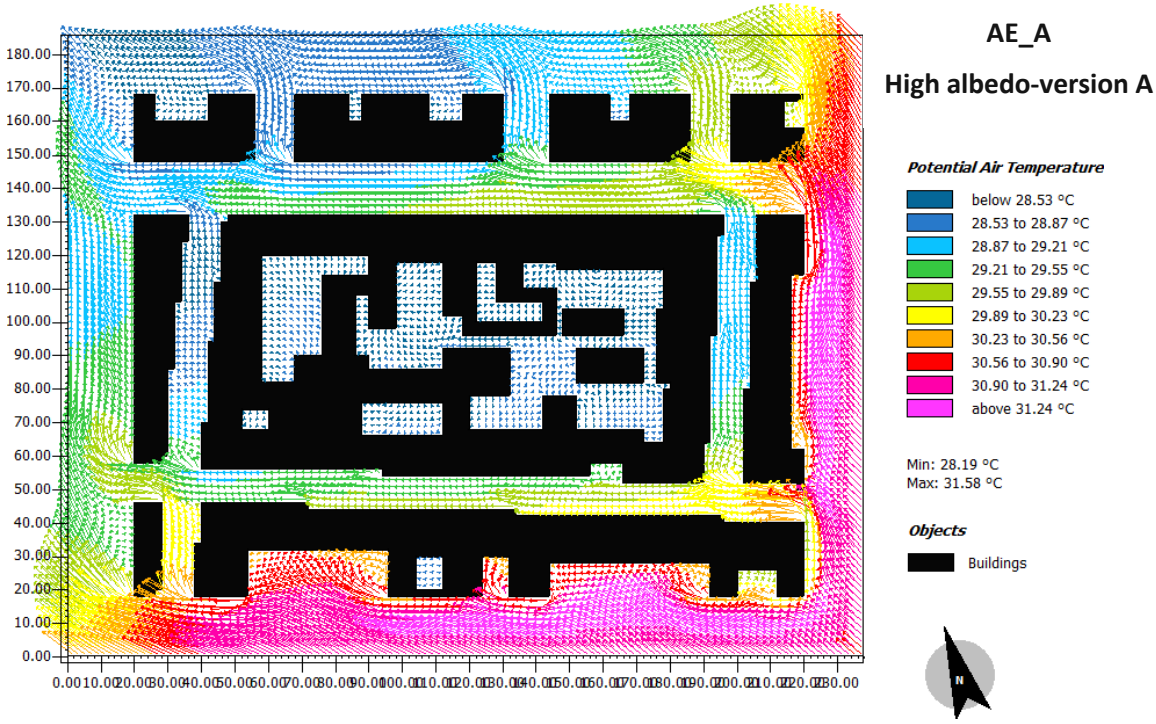

Figure 31. 2D map of AE_A

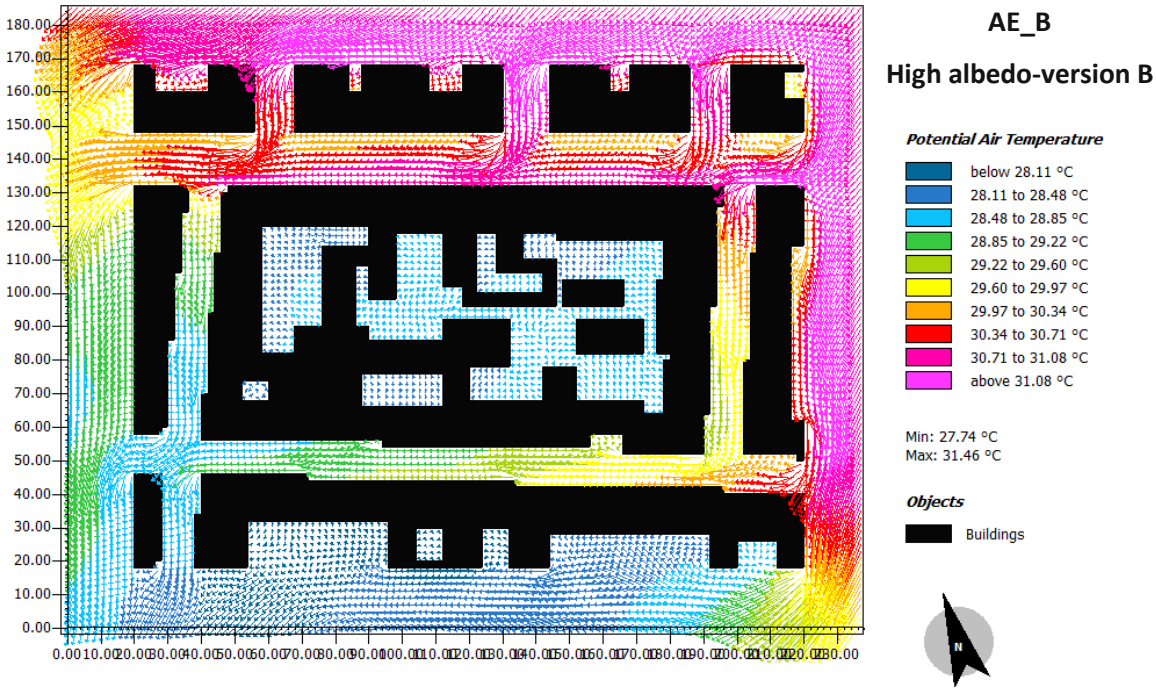

Figure 32. 2D map of AE_B

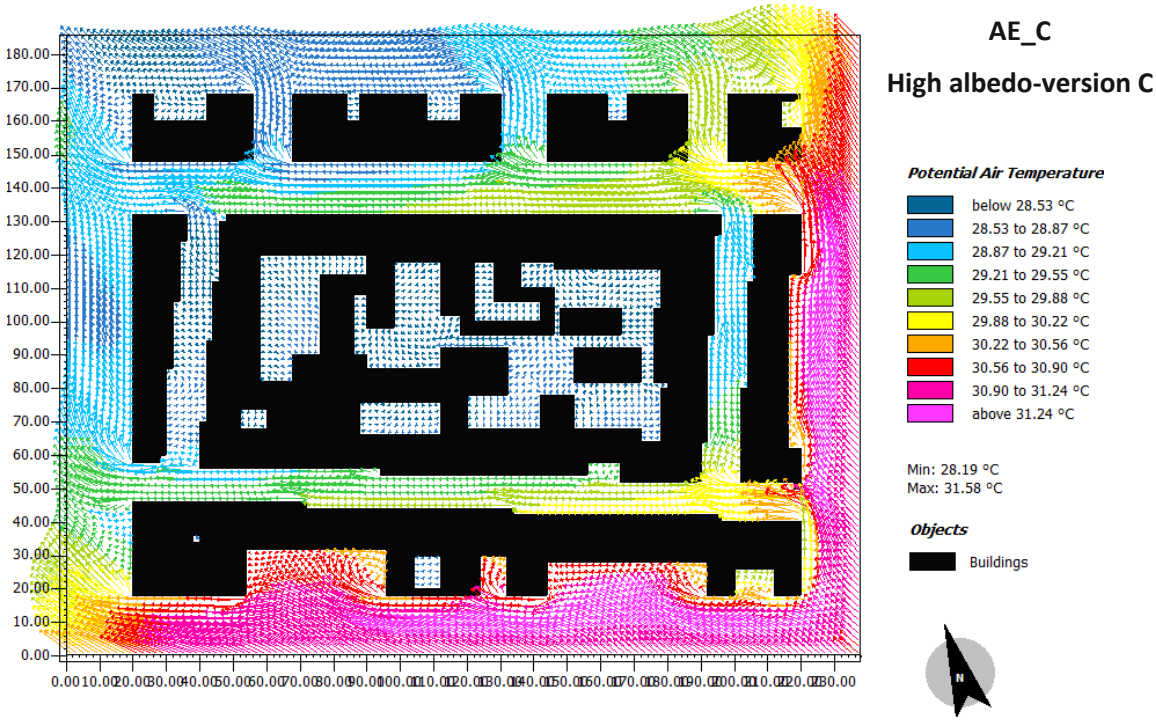

Figure 33. 2D map of AE_C

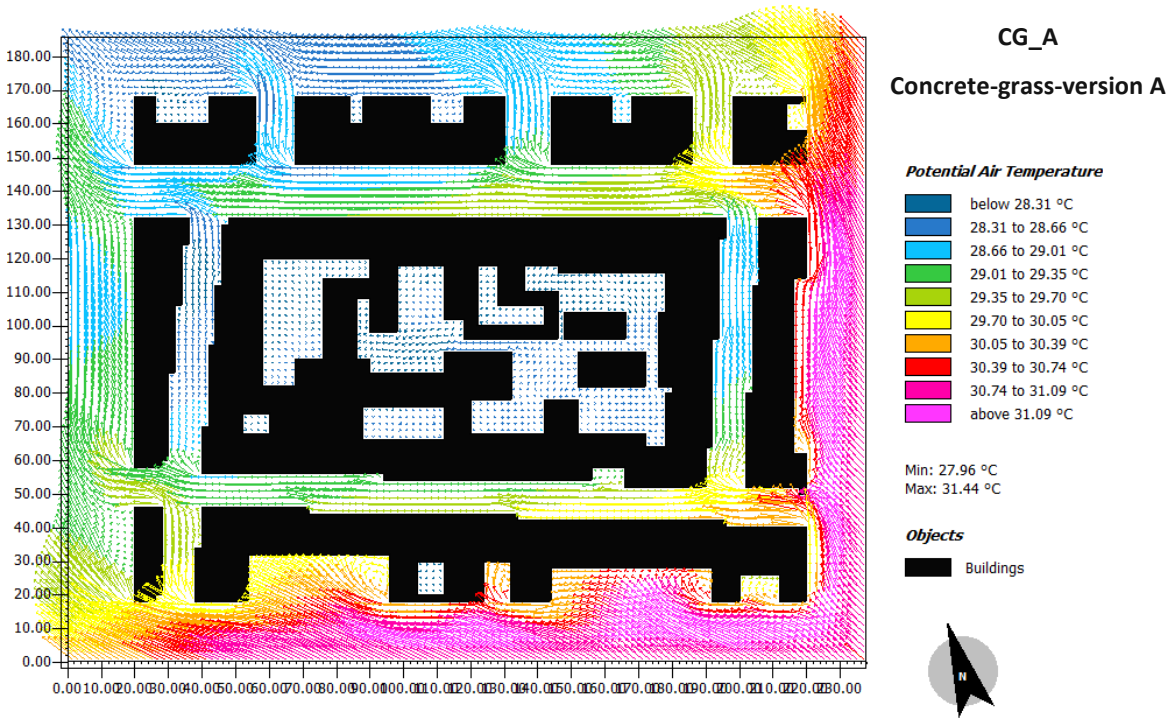

Figure 34. 2D map of CG_A

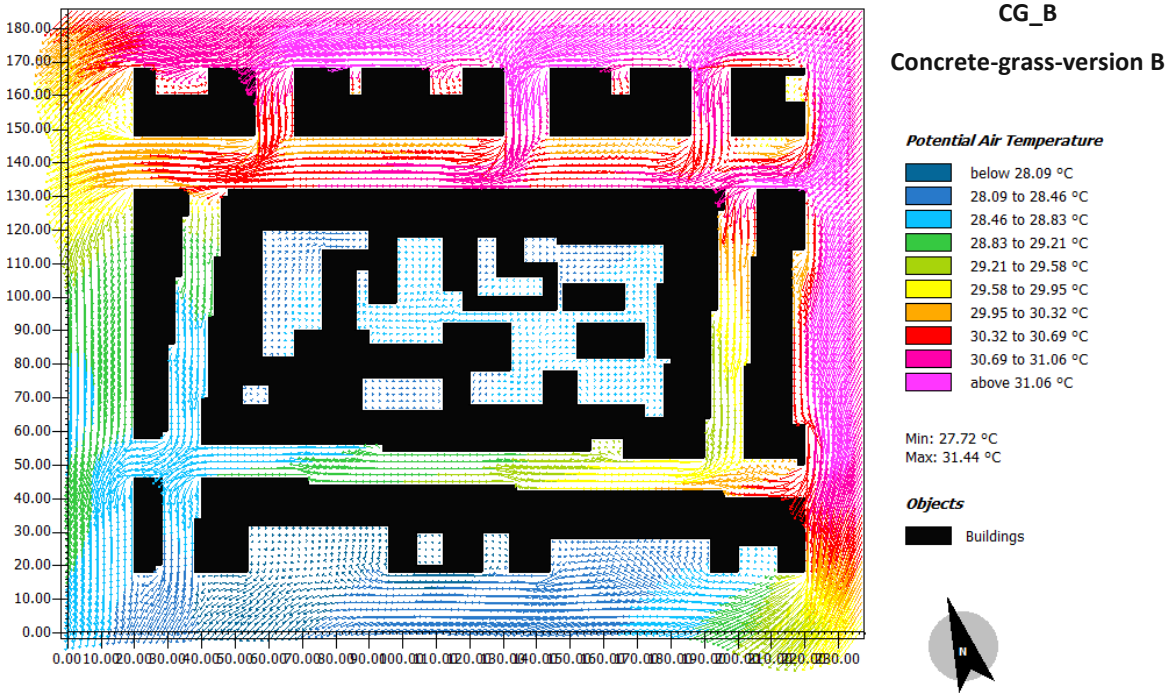

Figure 35 2D map of CG_B

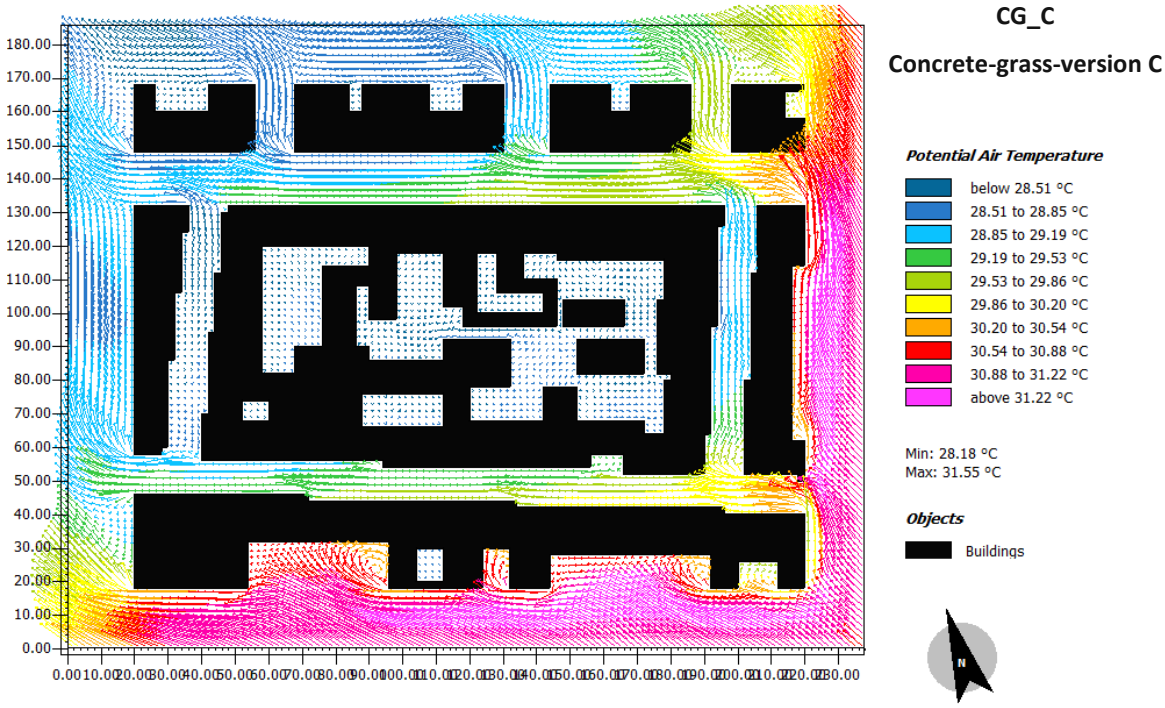

Figure 36 2D map of CG_C

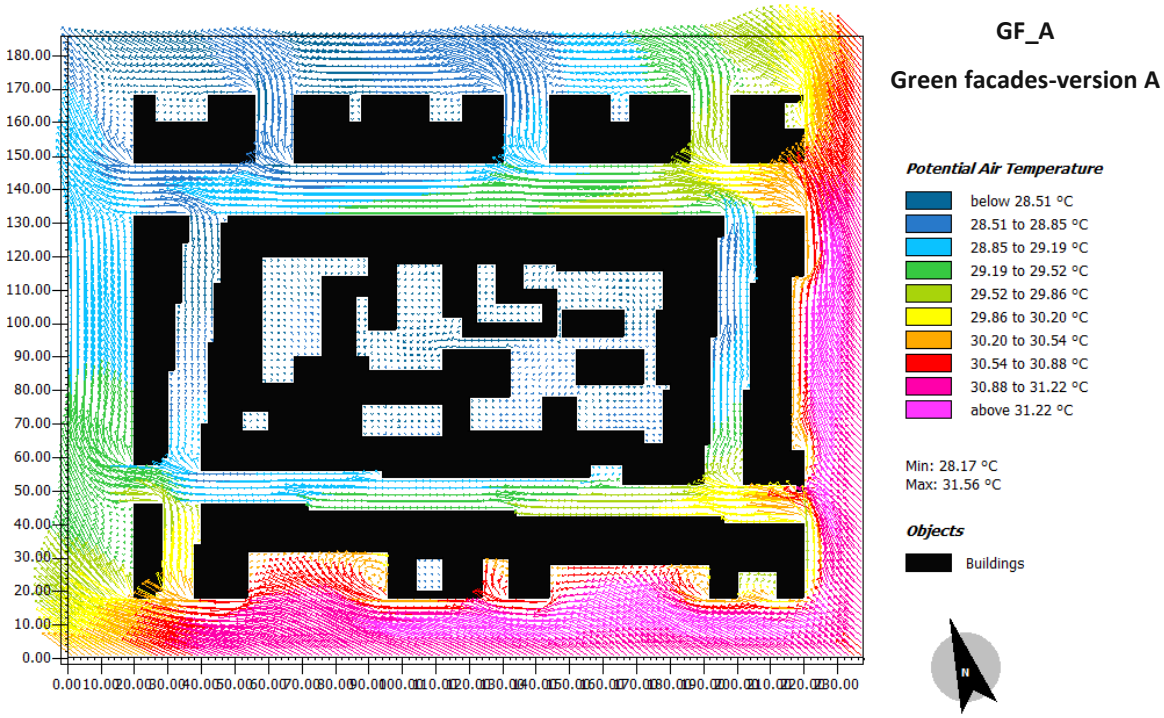

Figure 37. 2D map of GF_A

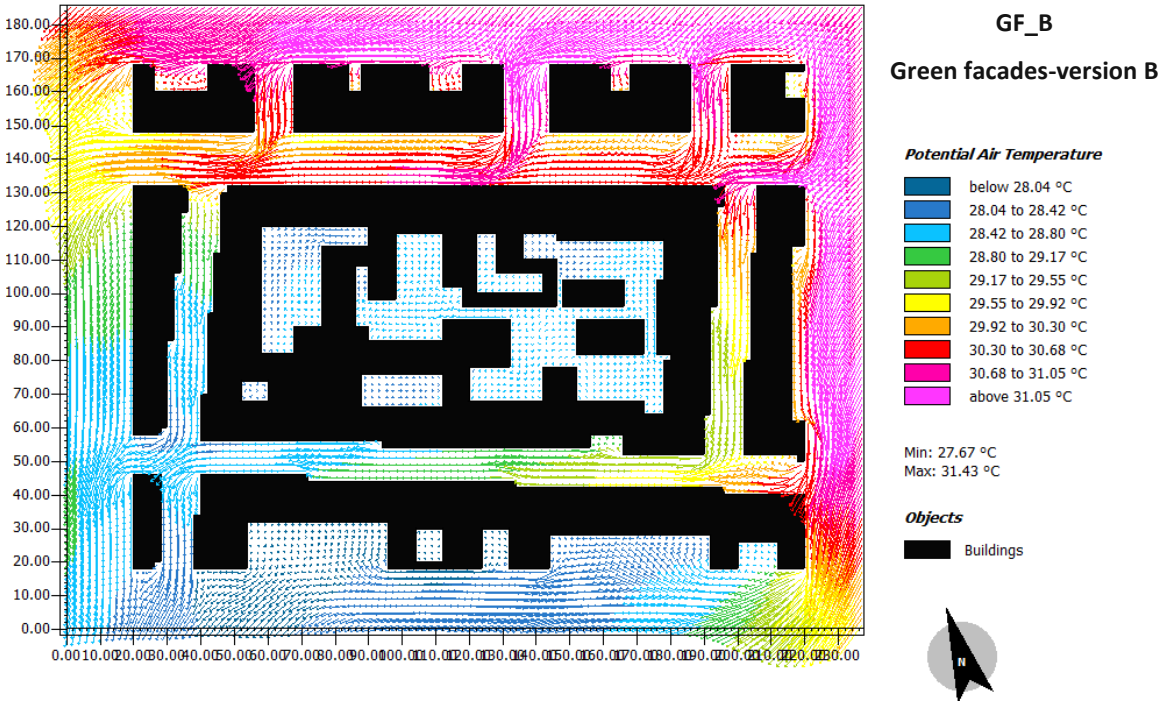

Figure 38. 2D map of GF_B

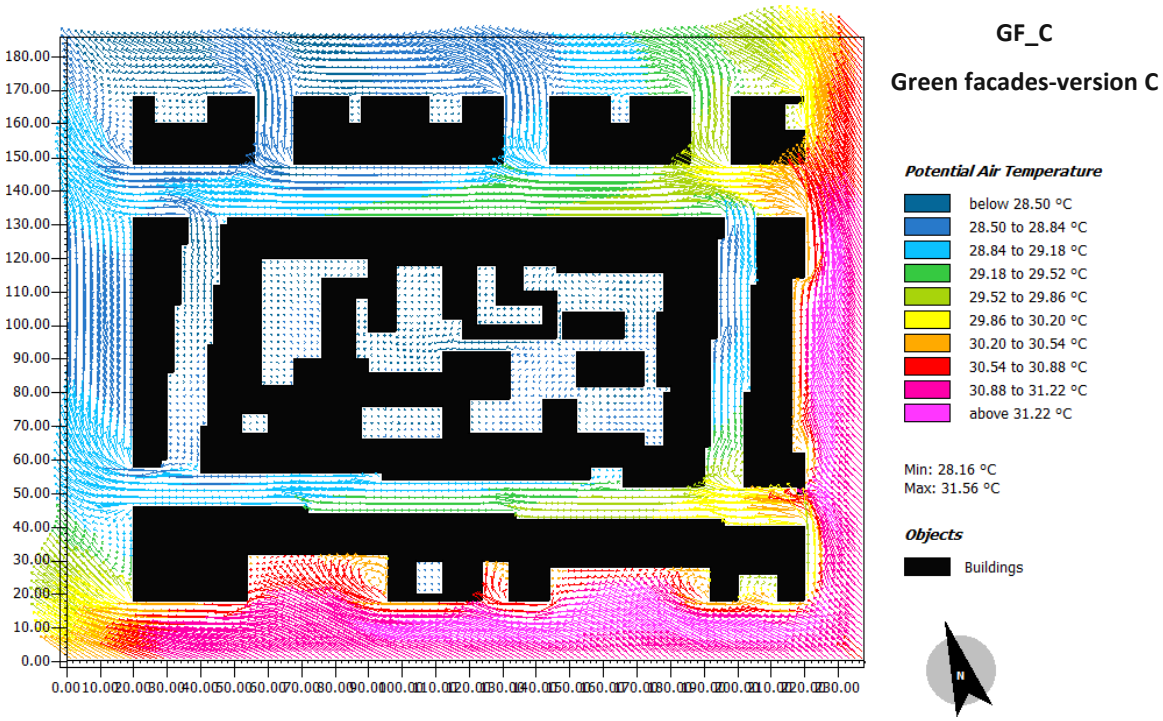

Figure 39. 2D map of GF_C

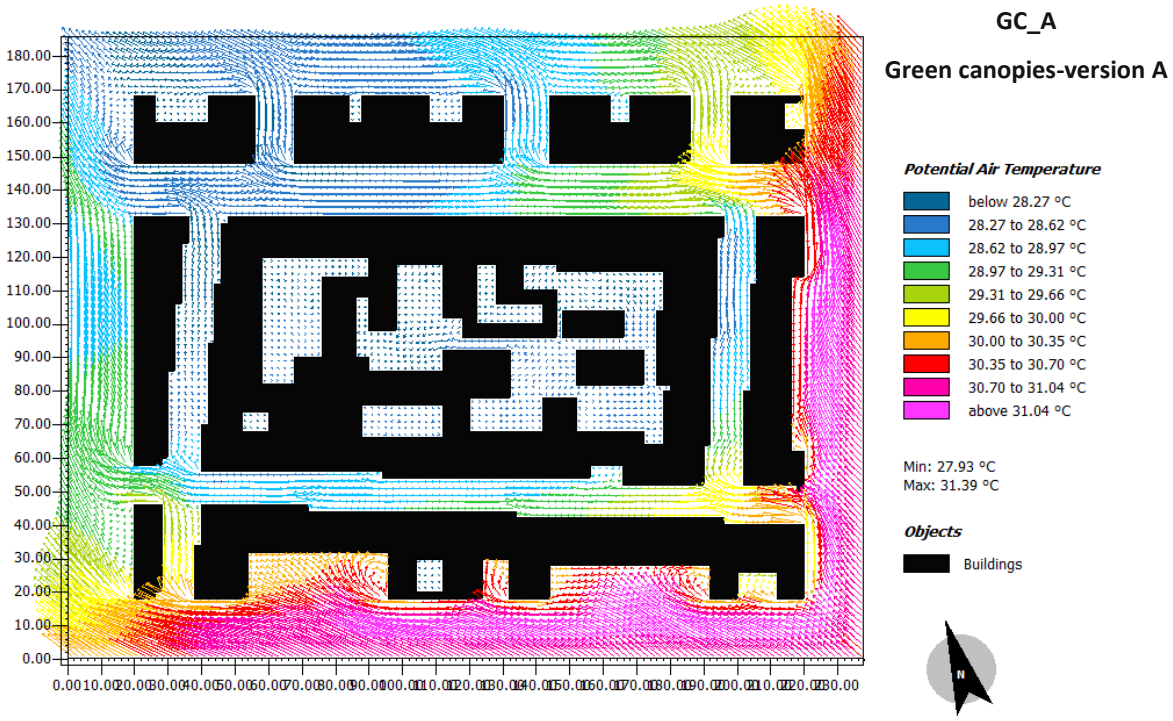

Figure 40. 2D map of GC_A

Figure 41. 2D map of GC_B

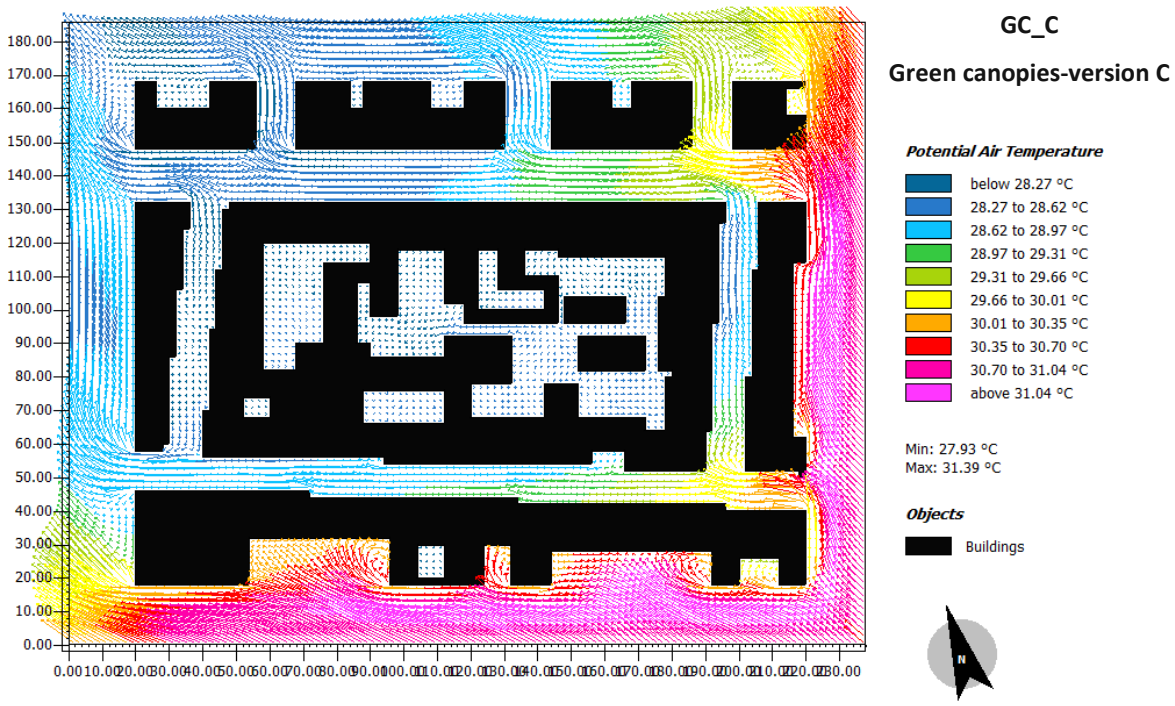

Figure 42. 2D map of GC_C

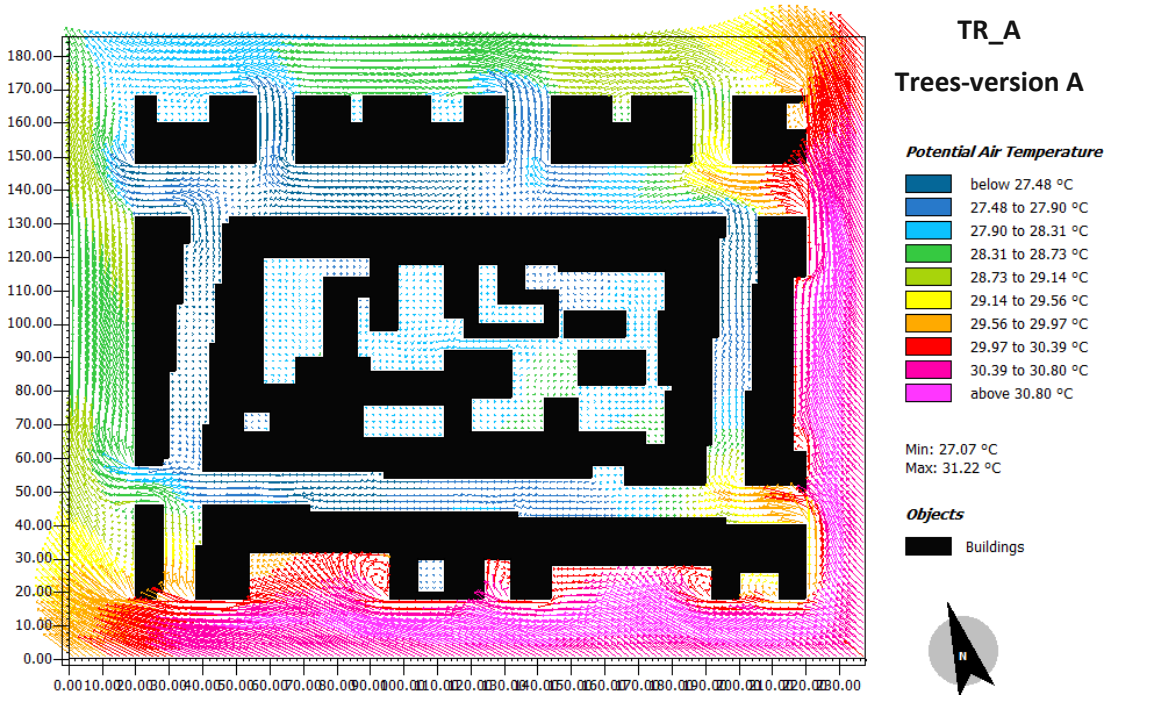

Figure 43. 2D map of TR_A

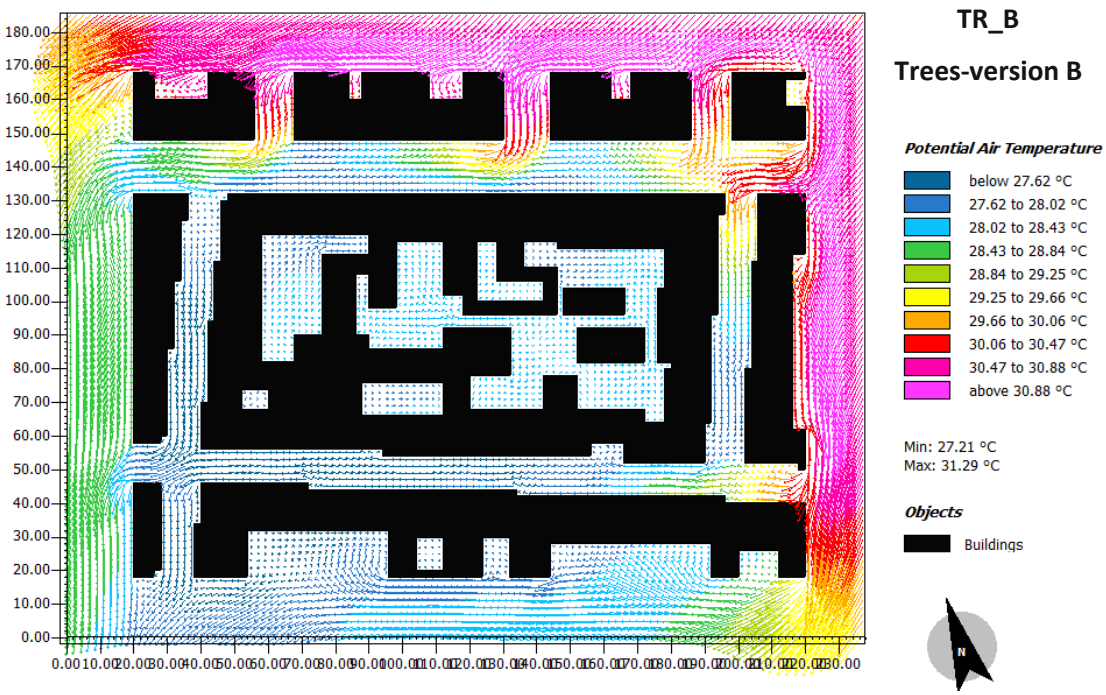

Figure 44. 2D map of TR_B

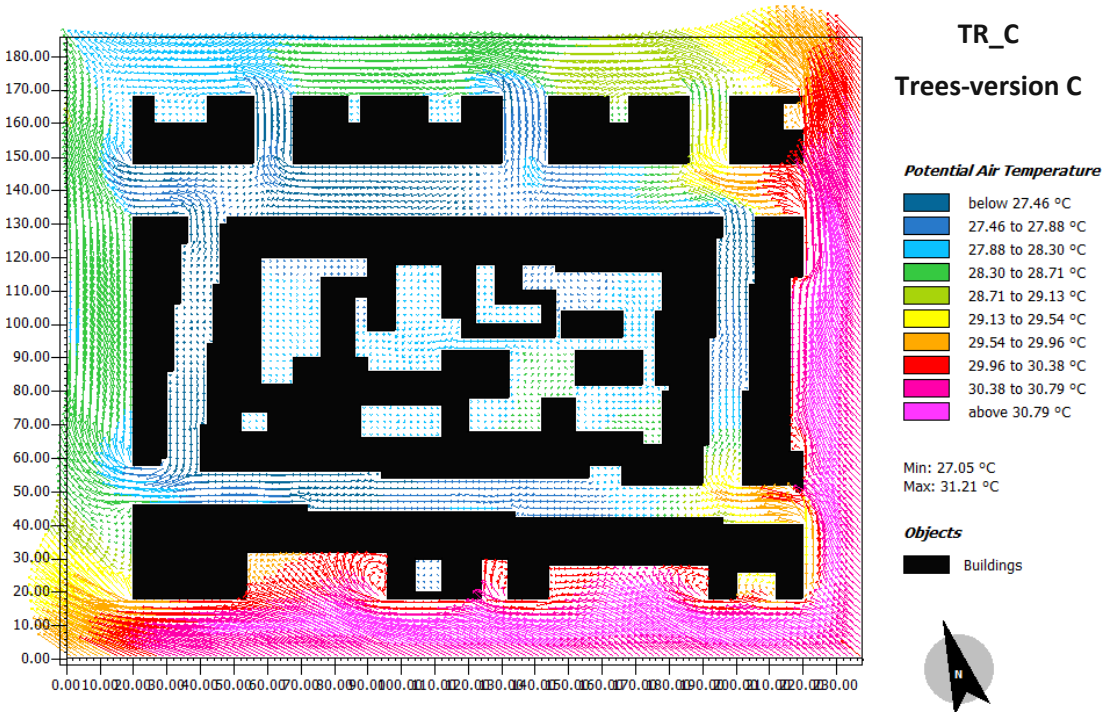

Figure 45. 2D map of TR_C

3.4 Graphs of streets' results at 2 pm

The graphs of detailed results of air temperature, wind speed and UTCI at height = 1.4m for Street_1, Street_2, Street_3 and Street_4 at 2 pm show the variations of microclimate between different urban canyons lying in the same region. The results are plotted for scenarios with versions A and B only since scenarios with version C have very similar air flow and temperature results to those with version A as shown in the 2D maps' section. The detailed results for relative humidity are not included since the humidity values are almost constant in all the scenarios with the three versions.

3.4.1 Air temperature results

In the temperature section the average temperature results of each street are plotted for the two existing site scenarios with versions A and B in 2D line graphs in Figure 46 and Figure 49. For other scenarios the temperature difference from the corresponding existing site scenario is plotted in box and whisker chart type as shown in Figure 47, Figure 48, Figure 50, and Figure 51.

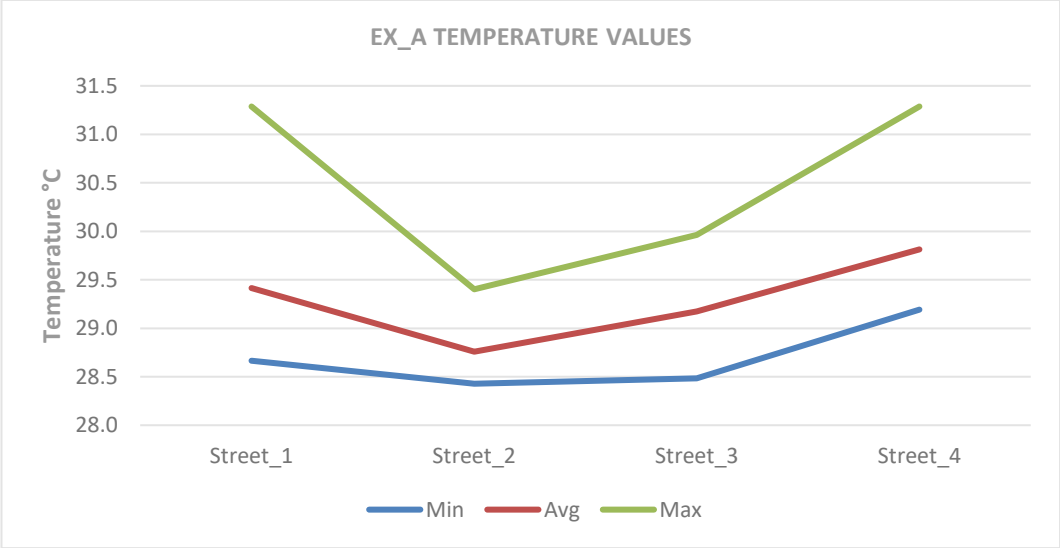

Figure 46. Temperature results for existing site scenario - Version A

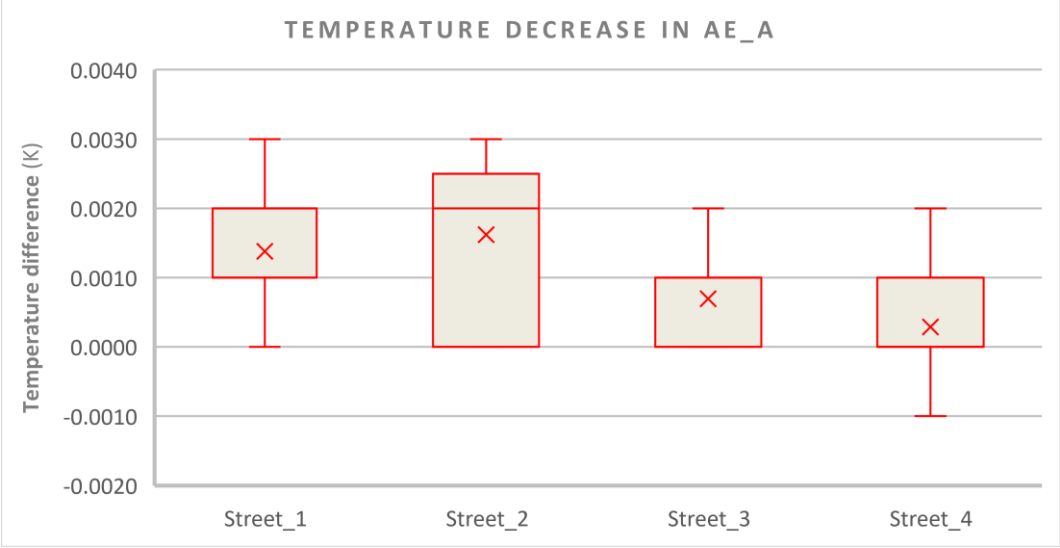

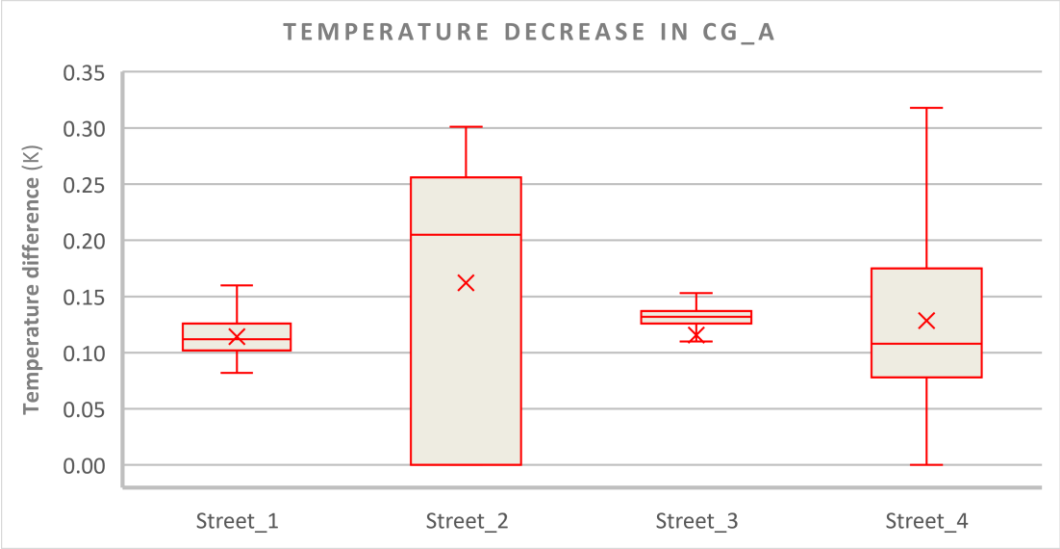

Figure 47. Temperature differences between EX_A and scenarios: AE_A and CG_A

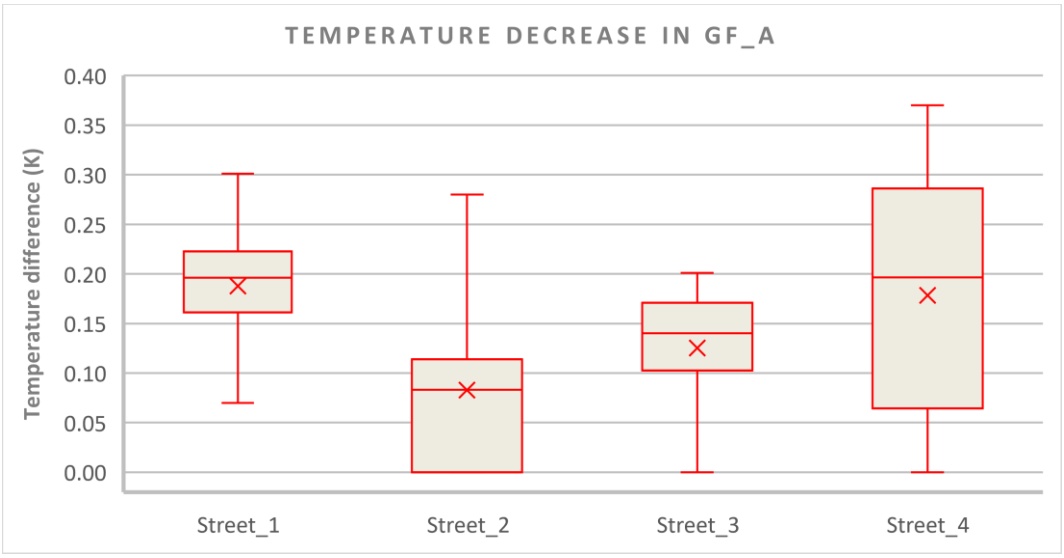

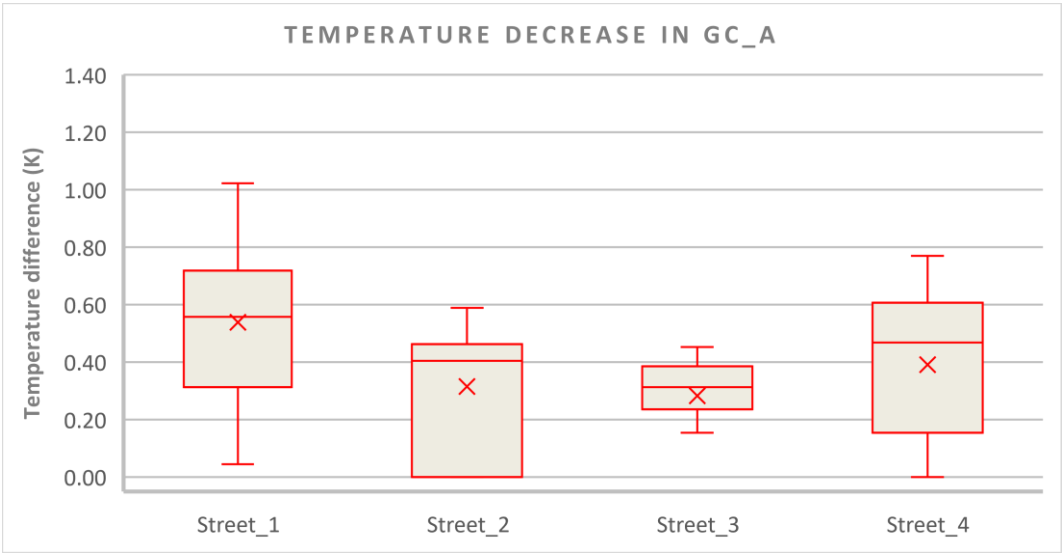

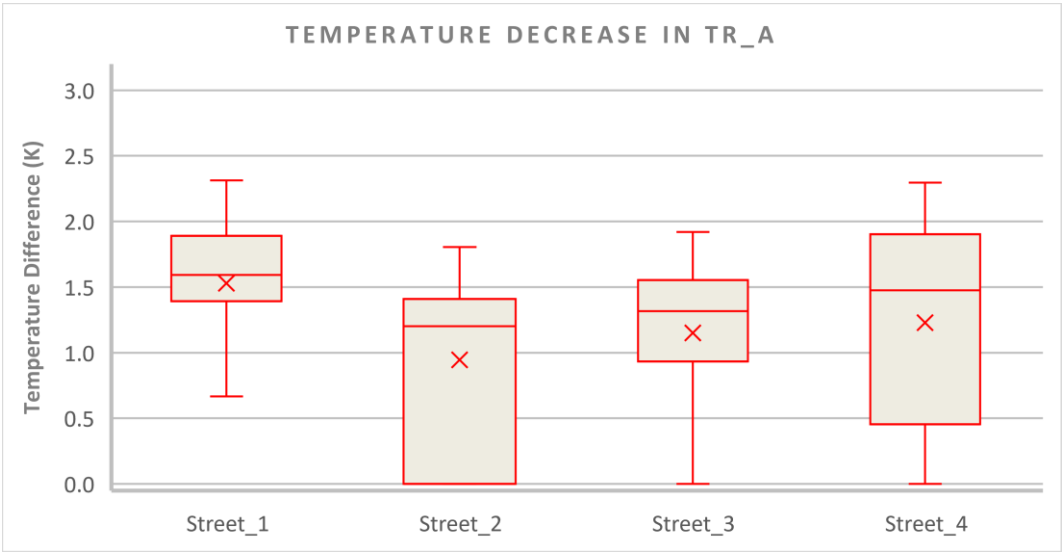

Figure 48. Temperature differences between EX_A and scenarios: GF_A, GC_A and TR_A

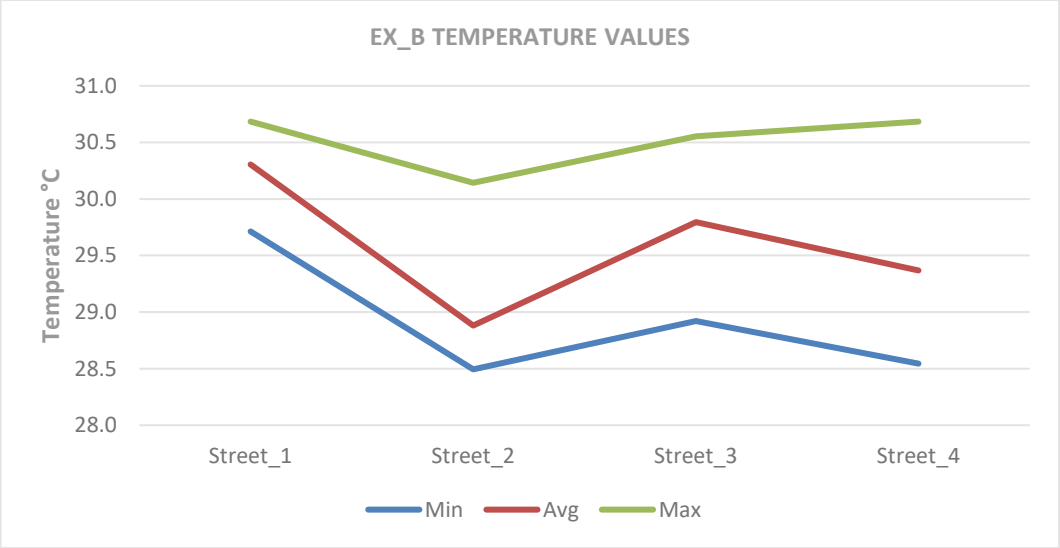

Figure 49. Temperature results for existing site scenario - Version B

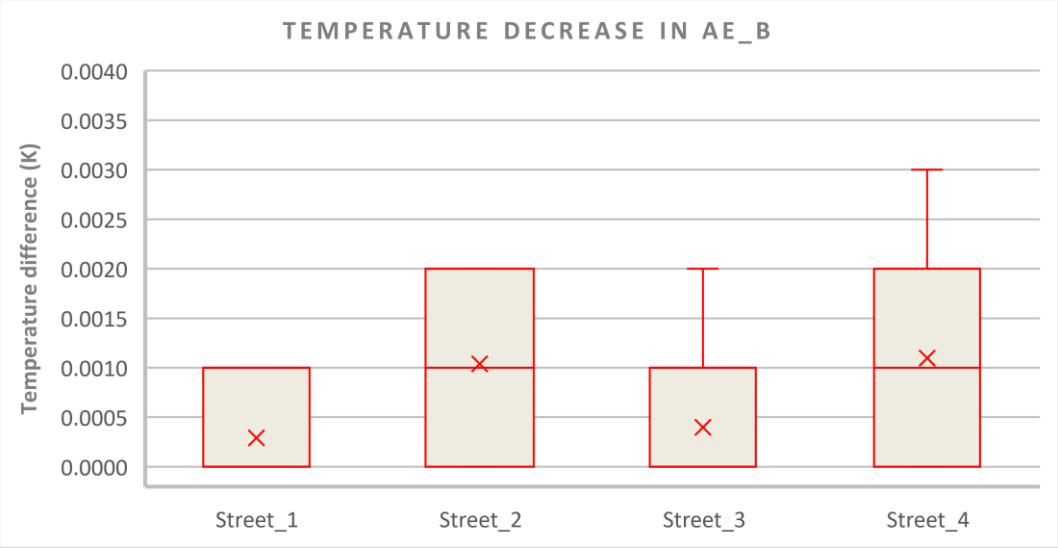

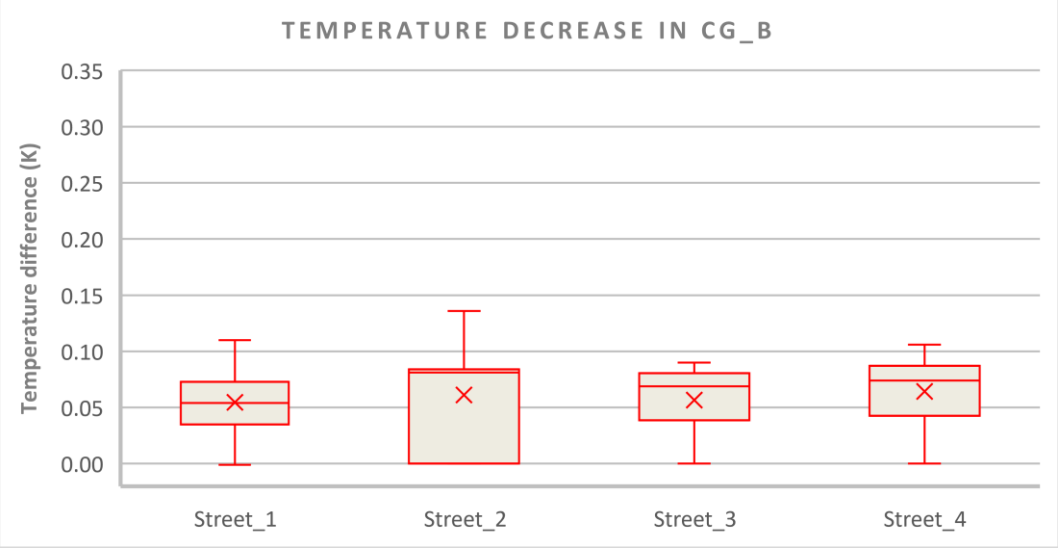

Figure 50. Temperature differences between EX_B and scenarios: AE_B and CG_B

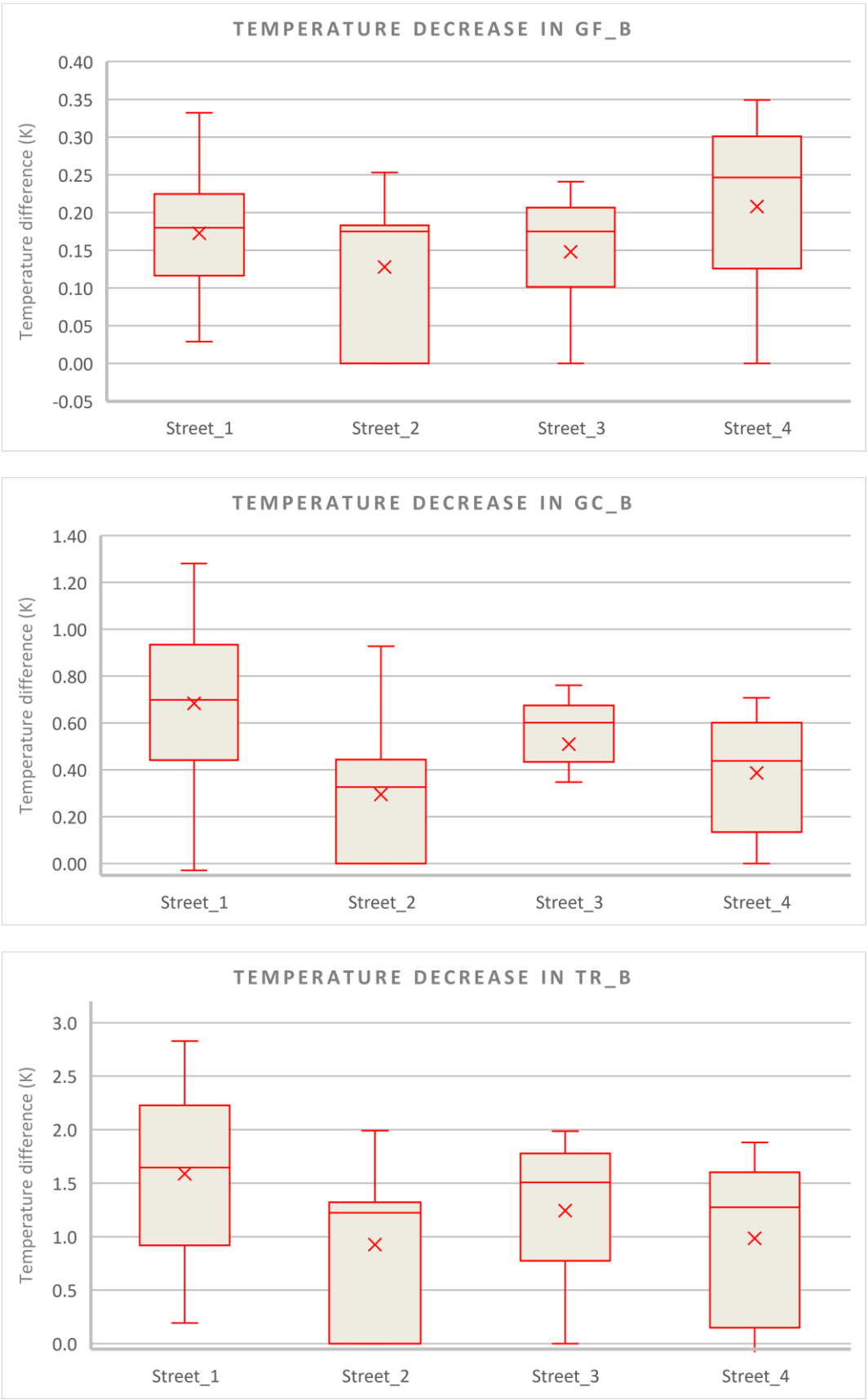

Figure 51. Temperature differences between EX_B and scenarios: GF_B, GC_B and TR_B

3.4.2 Wind speed results

The wind speed results of each street are plotted in 3D column chart type for each six scenarios with the same version as shown in Figure 52 and Figure 53.

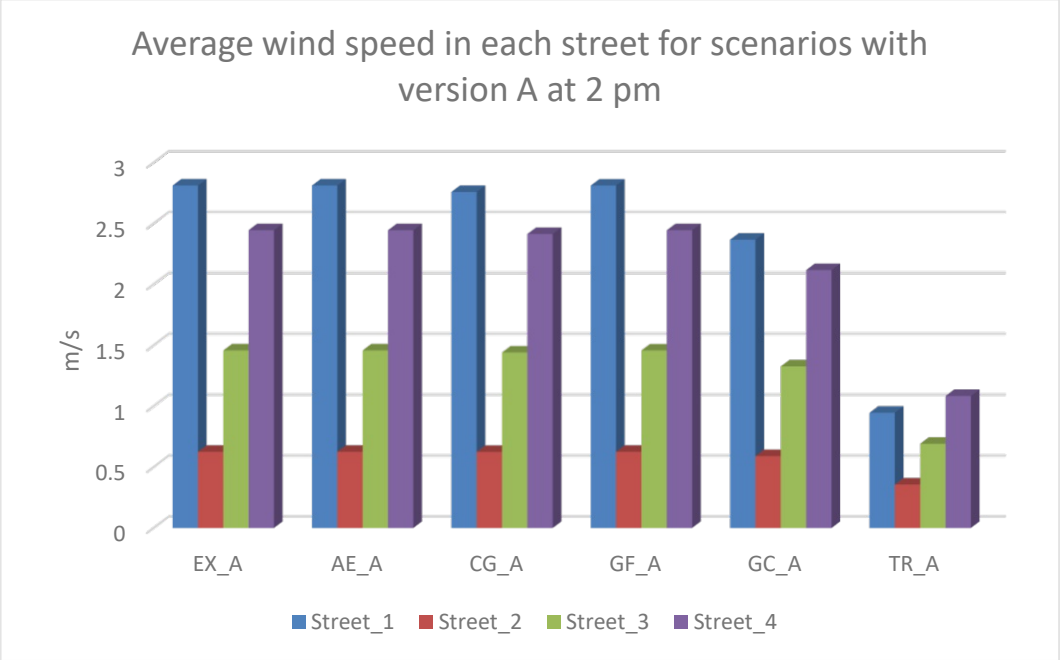

Figure 52. Average wind speed for Street_1, Street_2, Street_3 and Street_4 in EX_A, AE_A, CG_A, GF_A, GC_A and TR_A

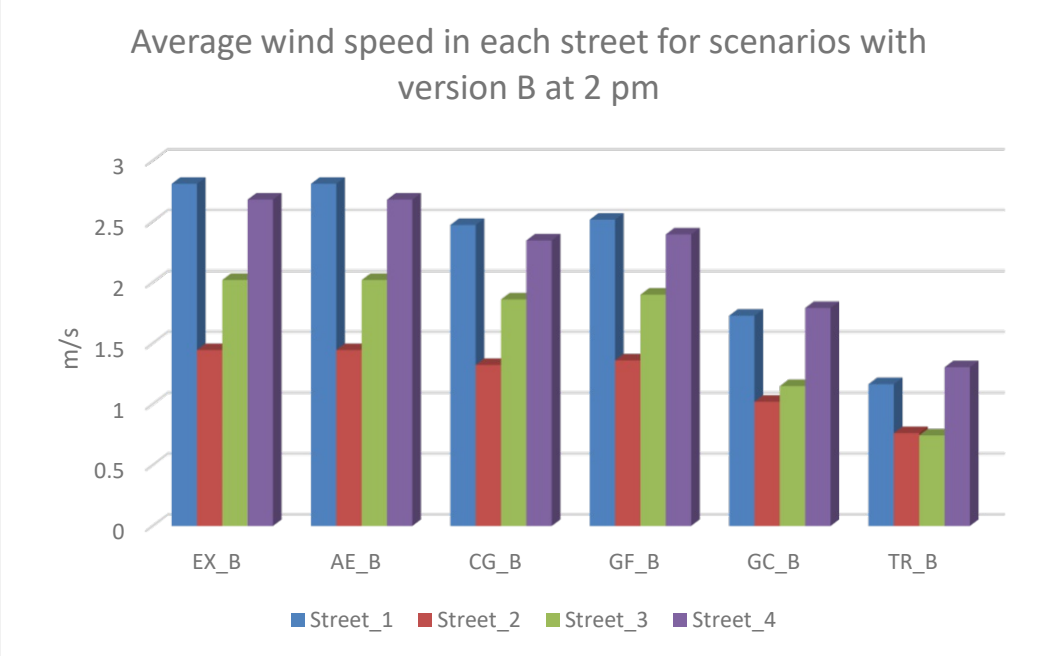

Figure 53. Average wind speed for Street_1, Street_2, Street_3 and Street_4 in EX_B, AE_B, CG_B, GF_B, GC_B and TR_B

3.4.3 UTCI results

The average UTCI of each street is plotted in 3D columns chart type for each six scenarios with the same version as shown in Figure 54 and Figure 55. Because the UTCI outdoor thermal comfort is calculated at wind speed higher than or equal 0.5, the percentage of cells where UTCI isn't calculated in the scenarios of green canopies and trees which have low wind speed results are included in Table 4 and Table 5. This step will give a better understanding for UTCI results in the different canyons.

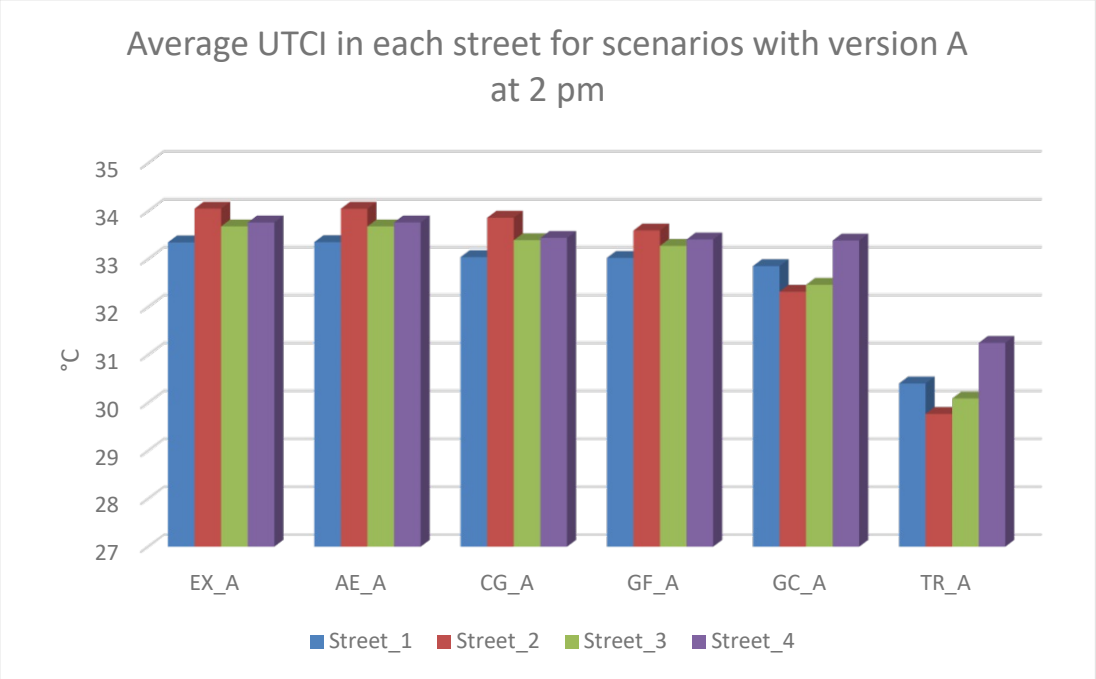

Figure 54. UTCI speed results for Street_1, Street_2, Street_3 and Street_4 in EX_A, AE_A, CG_A, GF_A, GC_A and TR_A

Table 4. Percentage of cells with version A where UTCI was not calculated in each street in green canopies' scenario (GC_A) and trees' scenario (TR_A) because UTCI cannot be calculated when air speed is < 0.5 m/s

	Version A			
	Percentage of cells where UTCI can't be calculated			
	Street_1	Street_2	Street_3	Street_4
GC_A (Green Canopies Scenario)	0.5%	52.0%	2.8%	3.1%
TR_A (Trees Scenario)	20.0%	81.0%	14.0%	22.0%

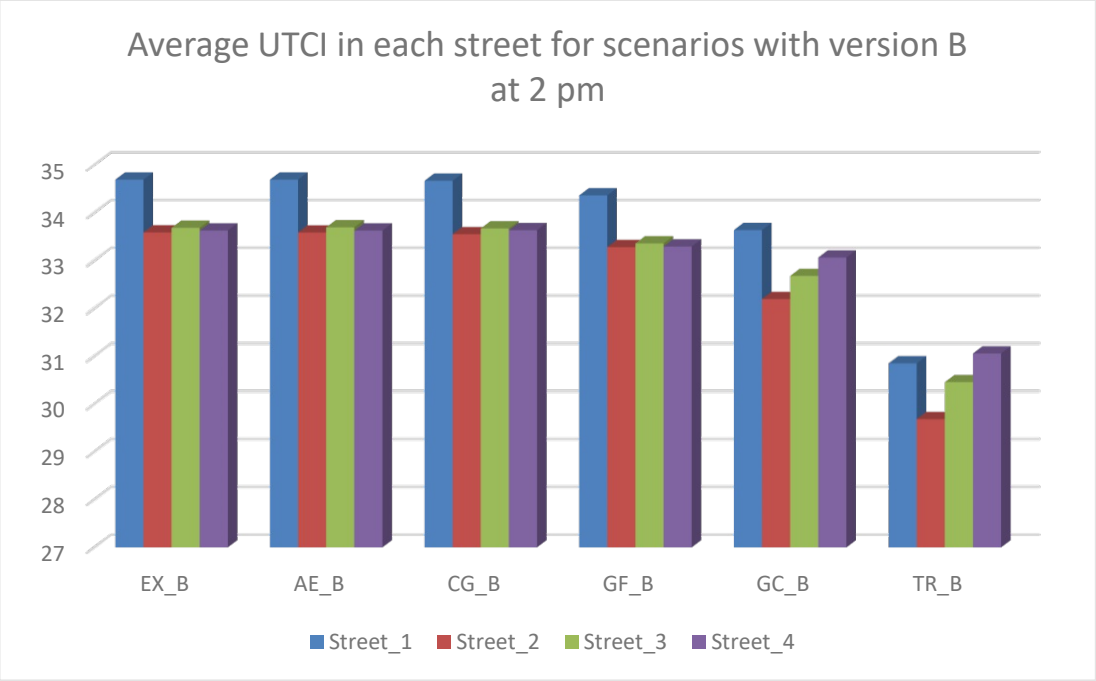

Figure 55. UTCI speed results for Street_1, Street_2, Street_3 and Street_4 in EX_B, AE_B, CG_B, GF_B, GC_B and TR_B

Table 5. Percentage of cells with version B where UTCI was not calculated in each street in green canopies' scenario (GC_B) and trees' scenario (TR_B) because UTCI cannot be calculated when air speed is < 0.5 m/s

	Version B			
	Percentage of cells where UTCI can't be calculated			
	Street_1	Street_2	Street_3	Street_4
GC_B (Green Canopies Scenario)	3.0%	13.3%	2.4%	2.8%
TR_B (Trees Scenario)	11.4%	25.0%	20.0%	5.3%

3.5 Mean radiant temperature graphs

Since the mean radiant temperature (Tmrt) depends on the direct radiation, reflected radiation and diffusive radiation and the wind direction has no impact on it, the results were plotted only for three scenarios with version A and precisely for the scenarios of existing site, green canopies, and trees (EX_A, GC_A, TR_A) as shown in Figure 55, where the two later scenarios imply shading which blocks a part of the direct solar radiation.

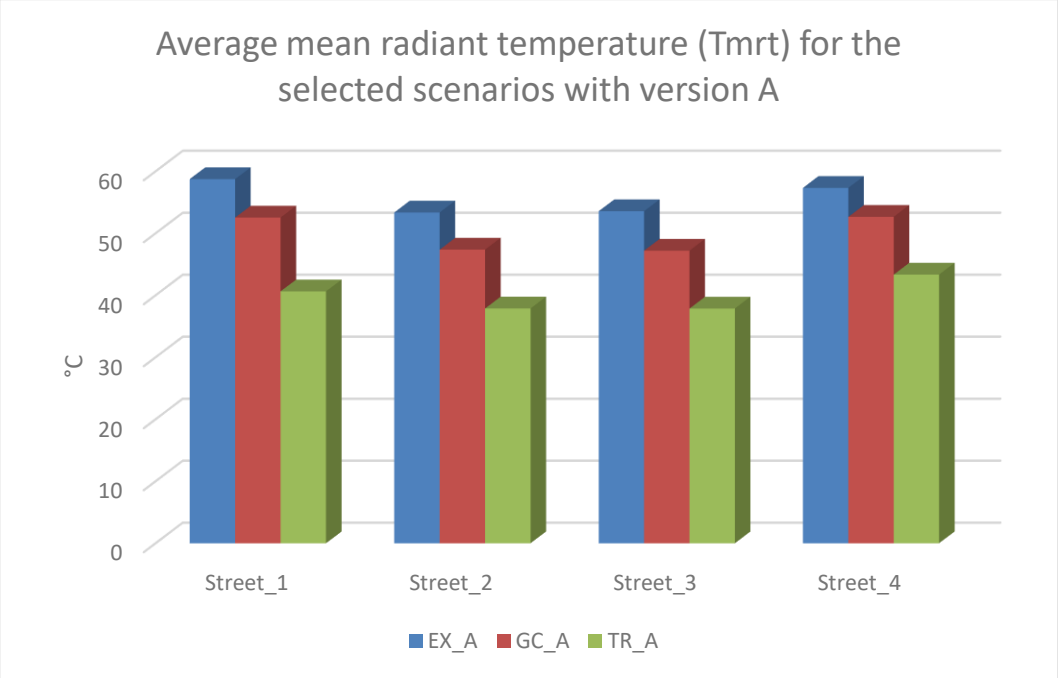

Figure 56. Mean radiant temperature results for the scenarios of existing site, green canopies, and trees with version A

3.6 Façade outside surface temperature

In order to evaluate the performance of the scenarios implying changes in the external walls of the building blocks (high albedo blocks and green facades), the outside surface temperature of a single cell in the middle of a façade of a building in Street_1 was calculated for 24 hours with version A for the scenarios of EX_A (existing site), AE_A (high albedo blocks) and GF_A (green facades) as shown in Figure 57. This evaluation will compare the impact of these changes on the microclimatic level to the buildings' level.

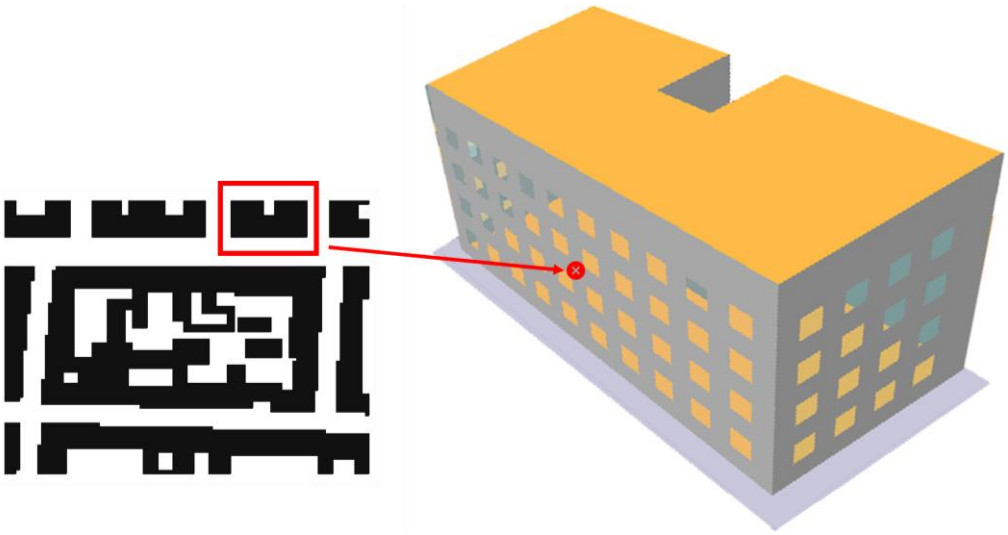

Figure 57. The selected cell of the chosen façade for plotting the outside surface temperature

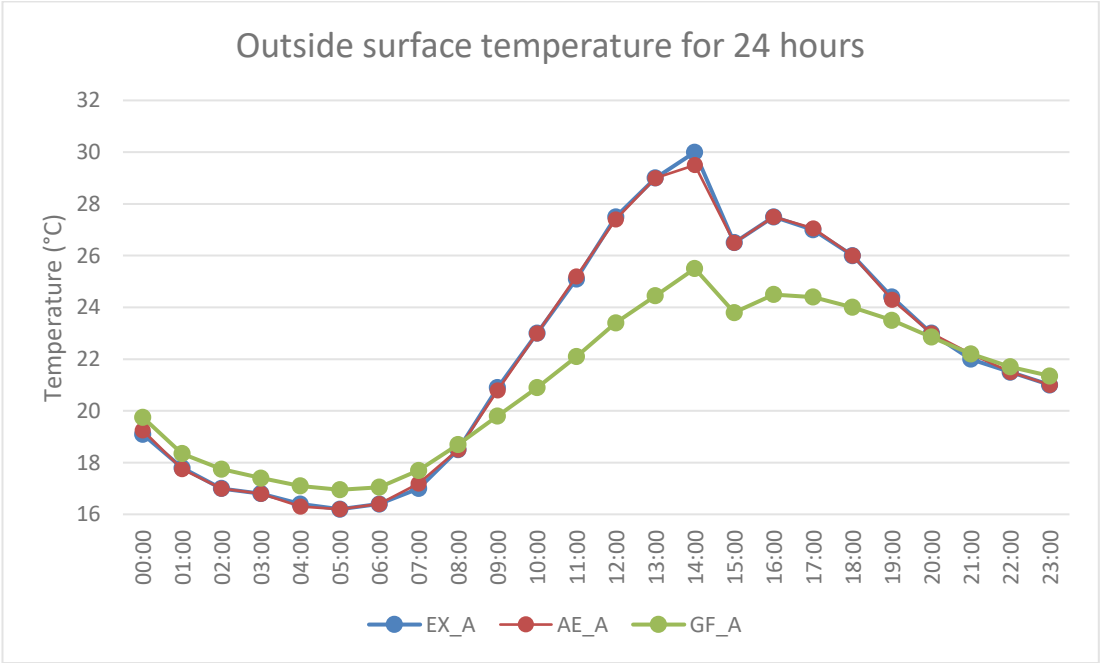

Figure 58. The outside surface temperature for 24 hours of the selected cell in the façade of a building in Street_1 with version A

4 DISCUSSION

In the discussion chapter, the aggregated results of the four streets for 24 hours and the detailed results for each street will be discussed separately.

4.1 Aggregated Results

The average temperature results showed a strong similarity in impact of the heat mitigation strategies in the three versions (Version A, Version B, Version C) as revealed in Figure 25. Temperature levels rise gradually from 6 am till they reach the peak at 2 pm In the six simulated scenarios with each version, only the green canopies scenario (GC) and trees scenario (TR) showed a notable variation in temperature. The deviation of temperature of these two mentioned scenarios from the existing site scenario (EX) starts increasing after 2 pm, which is the time of the peak temperature during the day. While the scenario of applying high albedo surface coating to the site blocks (AE) showed negligible shift in temperature results, also the strategies of concrete grass tiling grid (CG) for the parking lots and green facades (GF) have showed a maximum temperature decrease = 0.2 K during 2 pm.

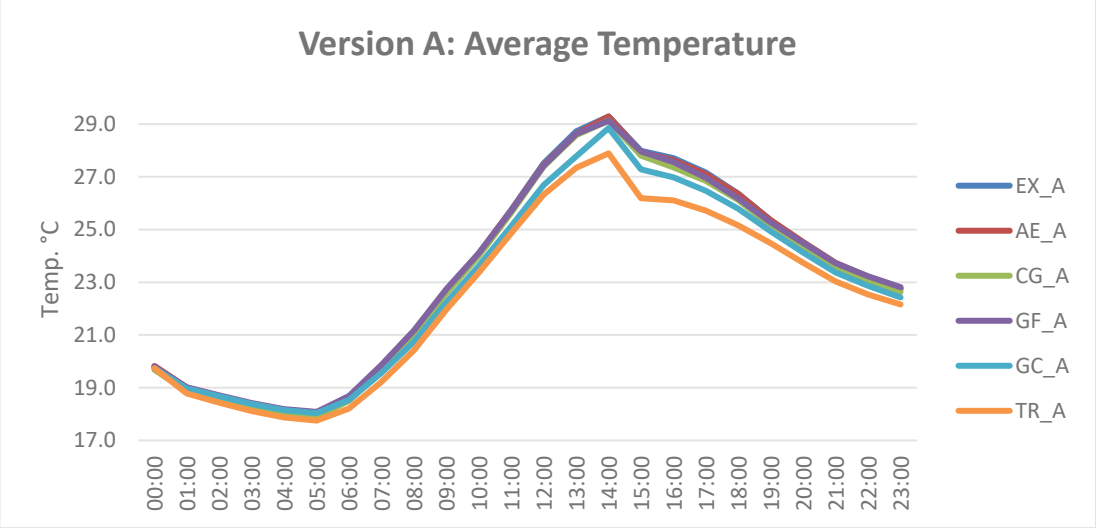

Figure 25 in page 21. Average temperature values for version A

The humidity levels in Figure 26 increase generally from 8 pm till 5 am. The lowest values occur at 2 pm. The relative humidity levels increased in all scenarios with applied vegetation (CG, GF, GC, TR). Only the high albedo scenario (AE) didn't provide any humidity variation from the existing site. The maximum rise in Humidity levels was in trees scenario (TR), which reached a 10% increase than the Existing site at 2 pm.

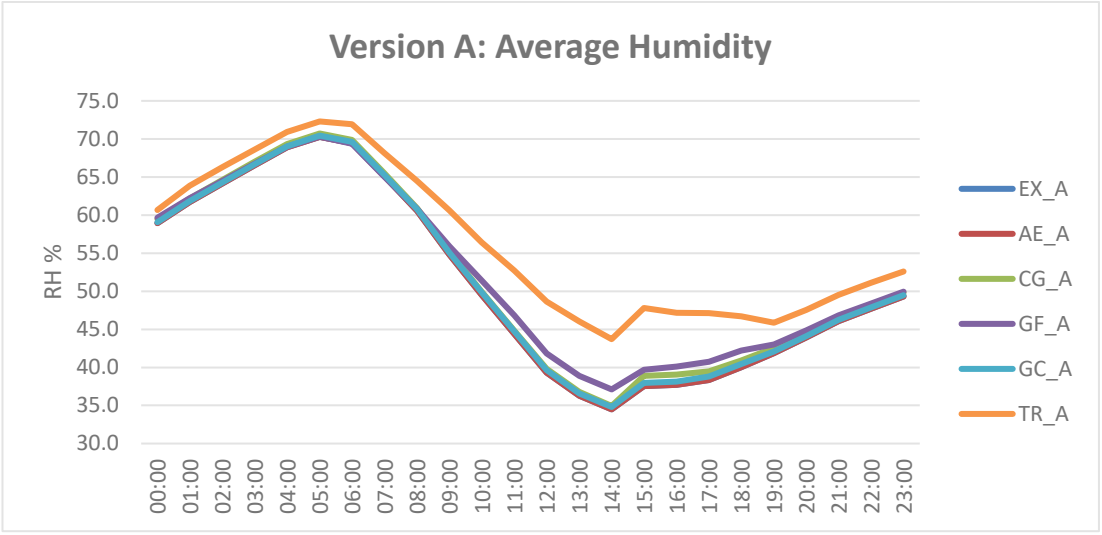

Figure 26 in page 22. Average relative humidity values for version A

The air speed shown in Figure 27 remained approximately constant in the existing site scenario (EX), high albedo blocks scenario (AE), concrete grass scenario (CG) and green facades scenario (GF). The green canopies scenario (GC) and trees scenarios (TR), which have vertical structures, have showed a remarkable average decrease in the wind speed values = 0.6 m/s and 1m/s respectively.

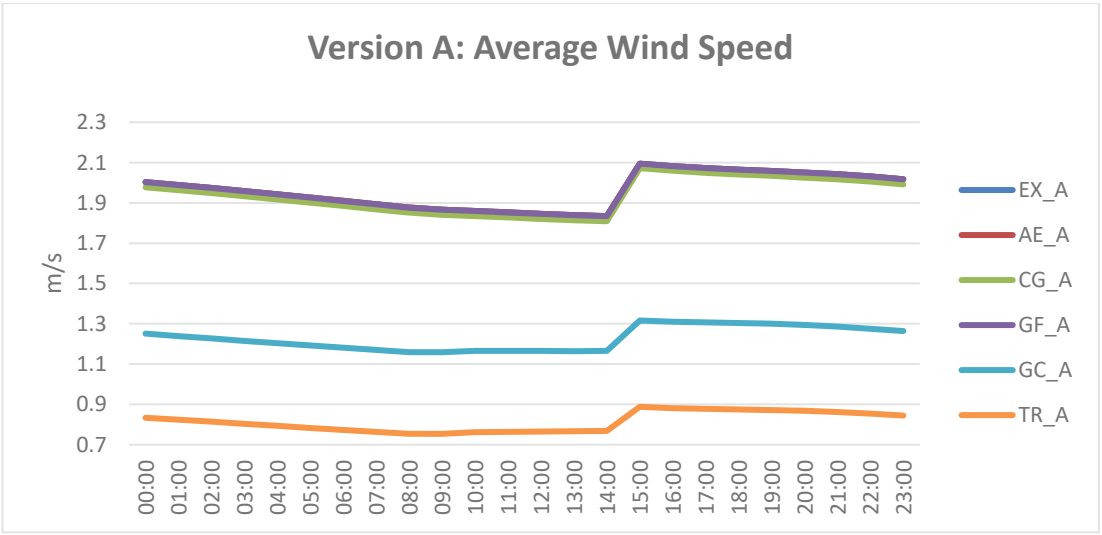

Figure 27 in page 23. Average wind speed values for version A

4.2 Streets' results at 2 pm

According to the 2D maps, the scenarios with version A and version C show a similarity in the results. The focus in this part will be on the comparison between scenarios with version A and version B, in which they have orthogonal wind directions.

4.2.1 Scenarios with version A

In scenarios with version A, temperature values are the highest in Street_1 and Street_4 according to the 2D maps in Figure 28 and Figure 29 and the plotted graph in Figure 34. This is probably due to that hot air from the boundaries access the site through Street_1 and Street_4 before the cooling effect of buildings' shading takes place. Street_1 has a slightly lower temperature values compared to Street_4 because it receives a cooled down airflow from Street_2 and Street_3. Street_2 has the least temperature values because it is the last urban canyon where air flows in, after it has been cooled down in street_4.

Figure 47 and Figure 48 reveal the decrease in temperature occurred in each scenario in version A. The high albedo blocks scenario (AE_A) had a negligible effect on the temperatures, while the concrete grass tiling (CG_A) in the parking lots led to an average temperature decrease = 0.15 K and the green facades scenario (GF_A) resulted in a temperature average decrease = 0.17 K. As expected, green canopies (GC_A) and trees (TR_A) due to their shading properties had the highest temperature reduction = 0.5 K and 1.2 K respectively. The cooling down effect of the vegetation strategies applied above the ground surface (GF_A, GC_A, and TR_A) is directly proportional to the air speed. Therefore, the mentioned vegetation strategies applied in Street_2 have a lower cooling effect compared to other streets. Figure 59 accumulates the temperature differences in each scenario (AE_A, CG_A, GF_A, GC_A, TR_A) from existing site scenario (EX_A).

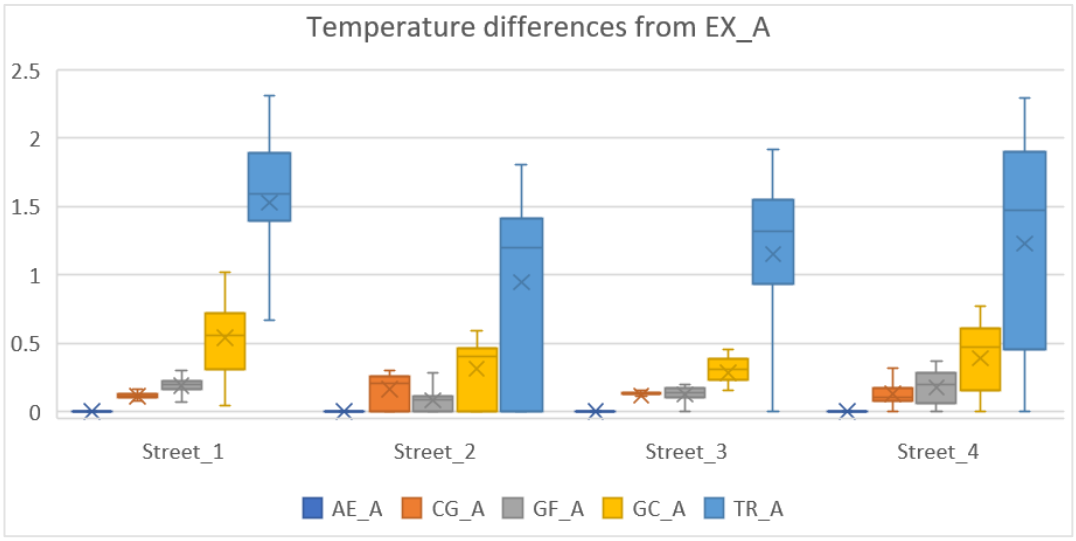

Figure 59. Accumulated temperature differences from EX_A for each street in each scenario with version A

In the air speed results shown in Figure 51, Street_2 had the lowest wind speed in all scenarios because air flow reaches Street_2 after being obstructed by the urban form. Another reason could be that it is easier for air flow to reach the simulation model outlet boundary surface through continuing in Street_4 instead of diverging to flow in Street_2. The green canopies and trees scenarios (GC_A and TR_A) are the effective strategies in air speed reduction. As an example, wind speed in Street_1 in the existing site scenario (EX_A) = 2.7 m/s, which went down to 2.3 m/s in green canopies scenario (GC_A) and then to 0.9 m/s in trees scenario (TR_A) as shown in Figure 51.

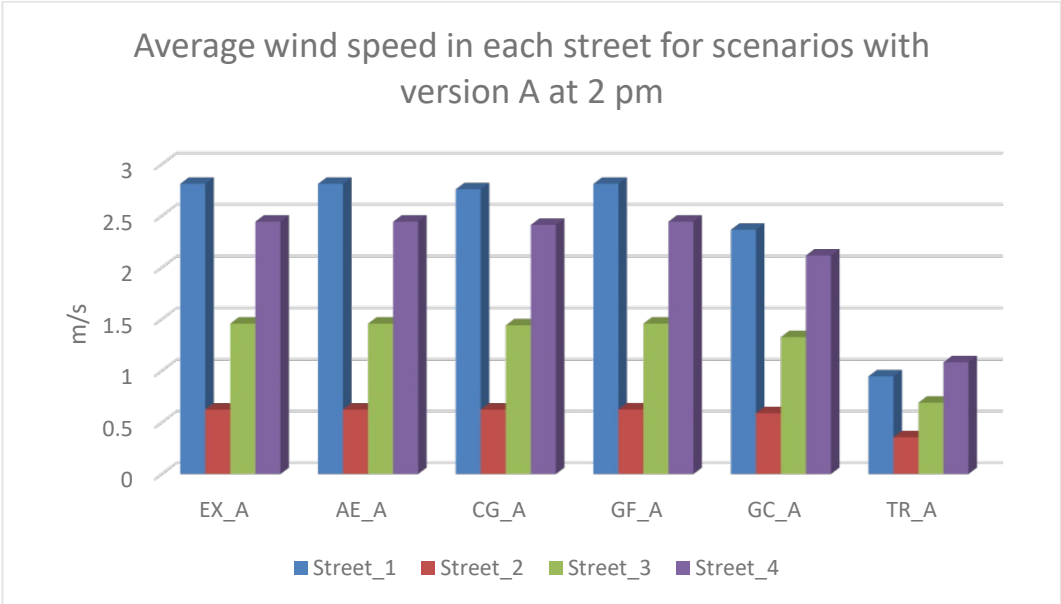

Figure 52 in page 40. Average wind speed for Street_1, Street_2, Street_3 and Street_4 in EX_A, AE_A, CG_A, GF_A, GC_A and TR_A

In the UTCI results shown in Figure 53, the scenarios of existing site (EX_A), concrete-grass grid (CG_A), green facades (GF_A), high albedo blocks (AE_A) and green canopies (GC_A) have values higher than 32, which is a strong heat stress zone. Trees scenario (TR_A) has an average UTCI = 30.6, which lies in the moderate heat stress zone. The UTCI value was maximum in Street_2 in the four scenarios of: existing site (EX_A), high albedo blocks (AE_A), concrete grass tiling grid (CG_A) and green facades (GF_A). While in the cases of green canopies and trees where shading is applied and mean radiant temperatures decrease considerably as shown in Figure 48, Street_2 has the lowest UTCI. As UTCI depends on the factors of air temperature, humidity, mean radiant temperature and wind speed, the dominance of each factor varies according to the circumstances. The reason why Street_2 has the lowest values in green canopies' and trees' scenarios (GC_A and TR_A) is that UTCI value can't be calculated at air speed less than 0.5m/s (Froehlich and Matzarakis, 2015). According to Table 4, UTCI wasn't calculated for 52% and 80% of cells of Street_2 in the scenarios of green canopies and trees (GC_A and TR_A) respectively because UTCI cannot calculated at wind speed less than 0.5 m/s. Therefore, the low UTCI values of Street_2 in the mentioned scenarios cannot be considered.

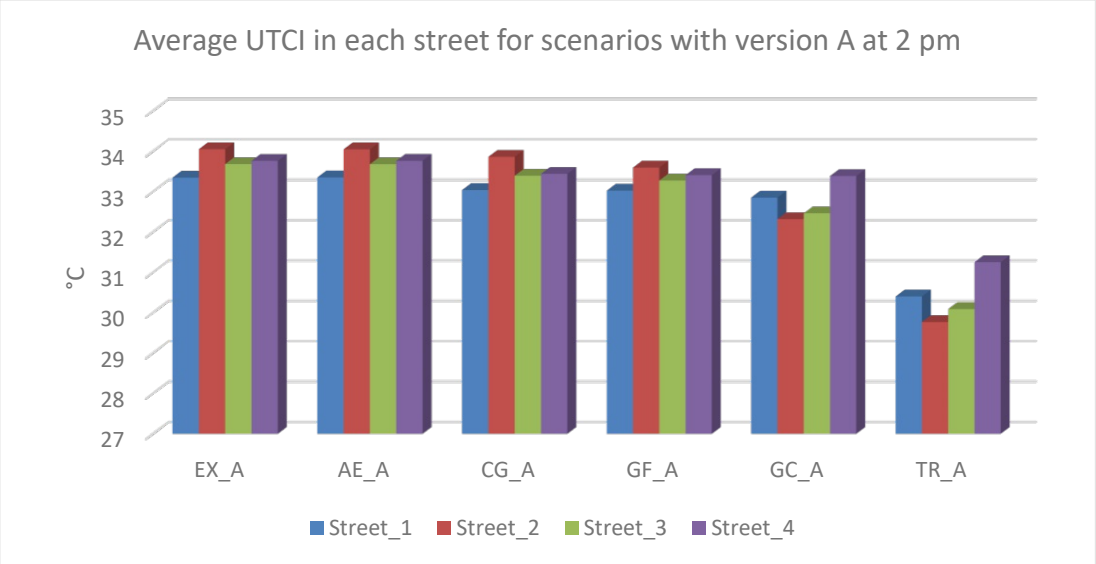

Figure 54 in page 41. UTCI speed results for Street_1, Street_2, Street_3 and Street_4 in EX_A, AE_A, CG_A, GF_A, GC_A and TR_A

Table 4 in page 41. Percentage of cells with version A where UTCI was not calculated in each street in green canopies' scenario (GC_A) and trees' scenario (TR_A) because UTCI can not be calculated when air speed is < 0.5 m/s

	Version A			
	Percentage of cells where UTCI can't be calculated			
	Street_1	Street_2	Street_3	Street_4
GC_A (Green Canopies Scenario)	0.5%	52.0%	2.8%	3.1%
TR_A (Trees Scenario)	20.0%	81.0%	14.0%	22.0%

4.2.2 Scenarios with version B

In scenarios with version B, temperature values are the highest in Street_1 and Street_3 according to the 2D maps in Figure 32 and Figure 33 and the plotted graph in Figure 37. This is probably due to that hot air from the boundaries access the site through Street_1 and Street_3 before the cooling effect of buildings' shading takes place. Street_1 has higher temperature values compared to Street_3 because it has hot airflow from four canyons, while in Street_3, air flows in only from Street_1.

Figure 49 and Figure 50 reveal the decrease in temperature occurred in each scenario with version B. The high albedo blocks scenario (AE_B) had a negligible effect on the temperatures, while the concrete grass tiling (CG_B) in the parking lots led to an average temperature decrease = 0.06 °K and the green facades scenario (GF_B) resulted in a temperature average decrease = 0.18 K. As expected, green canopies and trees (GC_B and TR_B) due to their shading properties had the highest temperature reduction = 0.5 K and 1.35 K respectively. The cooling down effect of the vegetation strategies applied above the ground surface (GF_B, GC_B, and TR_B) is directly proportional to the air speed. Therefore, the mentioned vegetation strategies applied in Street_2 have a lower cooling effect compared to other streets. Figure 60 shows the average temperature differences for each street in scenarios AE_B, CG_B, GF_B, GC_B and TR_B from the existing site scenario (EX_B).

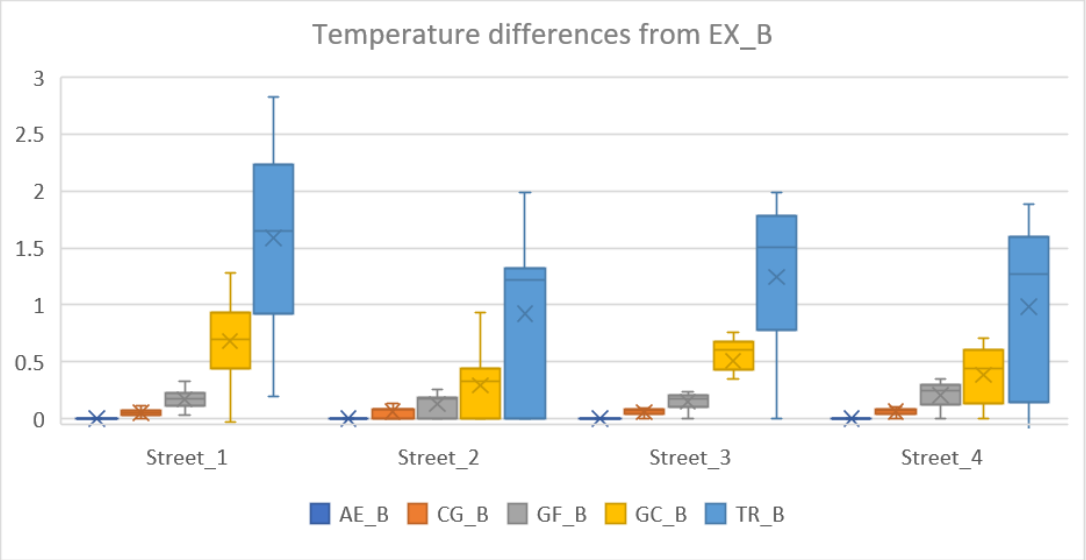

Figure 60. Accumulated temperature differences from EX_B for each street in each scenario with version B

In the air speed results shown in Figure 52, Street_2 had the lowest wind speed in all scenarios because air flow reaches Street_2 after being obstructed by the urban form. Another reason could be that it is easier for air flow to reach the simulation model outlet boundary surface through continuing in Street_1 instead of diverging to flow in Street_2. The green canopies' and trees' scenarios (GC_B and TR_B) are the effective strategies in air speed reduction. As an example, wind speed in Street_1 in the existing site scenario (EX_B) = 2.7 m/s, which went down to 1.6 m/s in green canopies scenario (GC_B) and then to 1.1 m/s in trees scenario (TR_B) as shown in Figure 52.

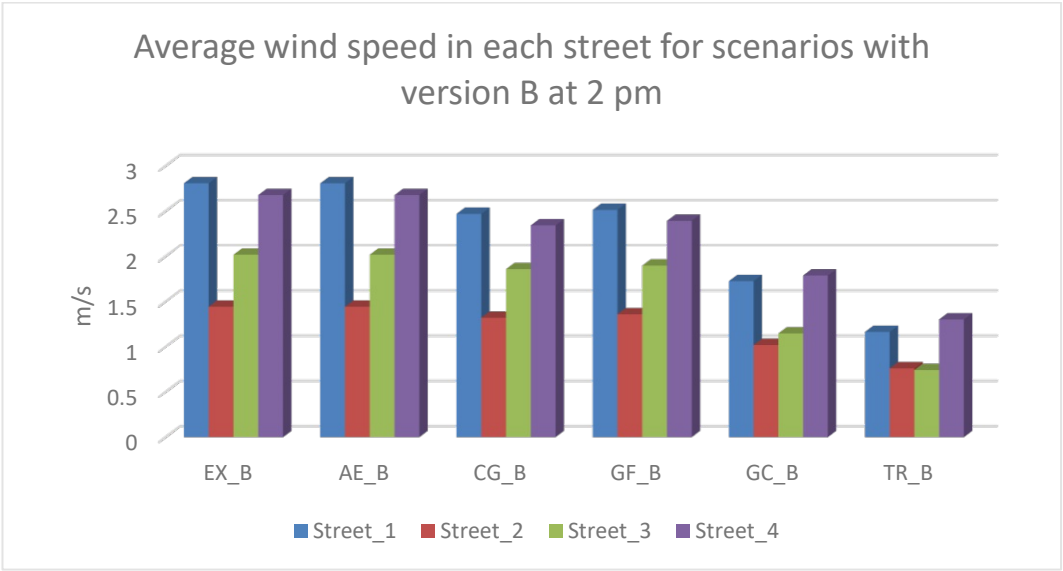

Figure 53 in page 40. Average wind speed for Street_1, Street_2, Street_3 and Street_4 in EX_B, AE_B, CG_B, GF_B, GC_B and TR_B

In the UTCI results represented in Figure 54, the scenarios of the existing site (EX_B), concrete-grass grid (CG_B), green facades (GF_B), high albedo blocks (AE_B) and green canopies (GC_B) have values higher than 32, which is a strong heat stress zone. Trees' scenario (TR_B) has an average UTCI = 30.6, which lies in the moderate heat stress zone. Street_1 and Street_4 have the highest UTCI values due to the high mean radiant temperatures they have. Figure 60 shows the average UTCI results for the four streets in the six scenarios with version B. Also, it should be considered that according to Table 5, UTCI wasn't calculated for 25% and 20% of cells of Street_2 and Street_3 in the scenario of trees (TR_B) because UTCI cannot be calculated at wind speed less than 0.5 m/s.

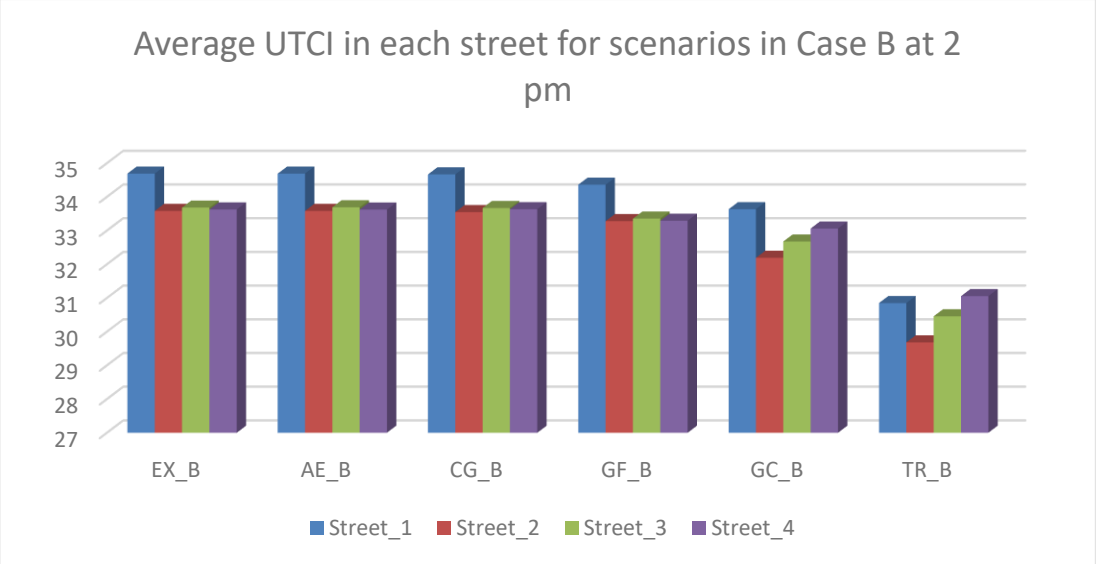

Figure 55 in page 42. UTCI speed results for Street_1, Street_2, Street_3 and Street_4 in EX_B, AE_B, CG_B, GF_B, GC_B and TR_B

Table 5 in page 42. Percentage of cells with version B where UTCI was not calculated in each street in green canopies' scenario (GC_B) and trees' scenario (TR_B) because UTCI can not be calculated when air speed is < 0.5 m/s

	Version B			
	Percentage of cells where UTCI can't be calculated			
	Street_1	Street_2	Street_3	Street_4
GC_B (Green Canopies Scenario)	3.0%	13.3%	2.4%	2.8%
TR_B (Trees Scenario)	11.4%	25.0%	20.0%	5.3%

4.3 Façade outside surface temperature

Because the scenarios where changes took place in building facades (green facades and high albedo facades) had a less impact on the heat mitigation compared to other scenarios, the outside surface temperature was calculated for a single cell in the middle of a façade of a building block in Street_1 in scenarios with version A as illustrated in Figure 49. The results in Figure 50 showed that the high albedo block (AE_A) had an outside surface temperature = 29.5°C which is 0.5 K lower than the outside surface temperature in the existing site scenario (EX_A). In the green facades' scenario (GF_A), the outside surface temperature = 25.5 °C, which is 4.5 K lower than that in the existing site scenario. Figure 57 illustrates the outside surface temperature for the three mentioned scenarios for 24 hours.

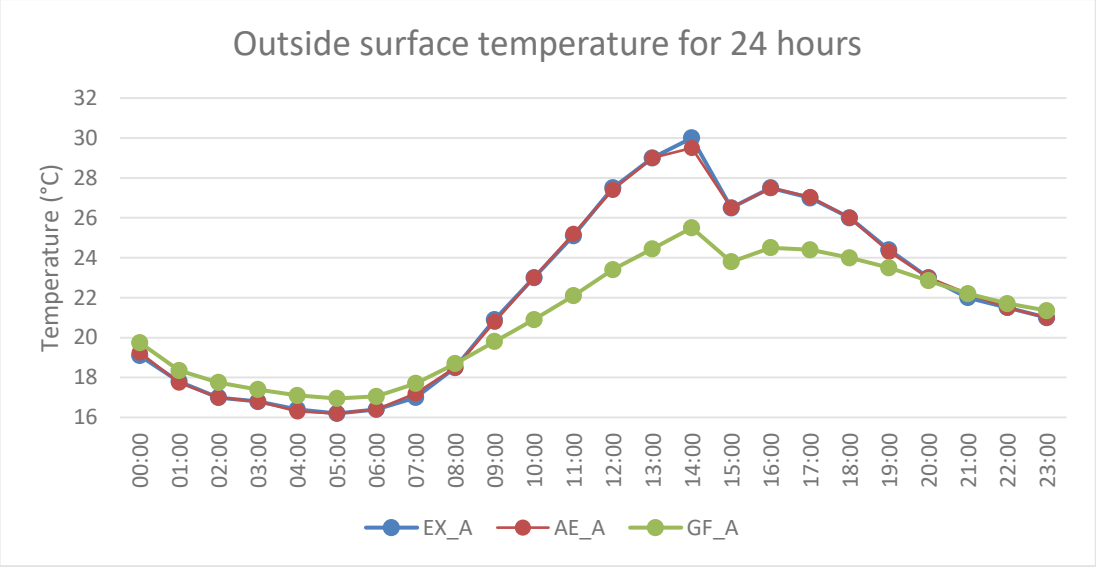

Figure 58 in page 43. The outside surface temperature for 24 hours of the selected cell in the façade of a building in Street_1 with version A

5 CONCLUSION

The results of the existing site scenarios with both versions A and B showed the impact of streets layout on the microclimate. The layout defines the air flow pattern in the site determining the air temperature and wind speed for each urban canyon.

The High Albedo blocks' scenarios (AE) had a negligible impact on the microclimate. The scenarios implying shading such as green canopies (GC) and trees (TR) have a stronger effect on the air temperatures compared to the strategies depending only on vegetation. The materials applying vegetation without shading can affect the thermal comfort negatively because they contribute positively to humidity levels in a much higher way than they decrease the air temperatures. Air speed is directly proportional to the evapotranspiration effect made by the vegetation.

In the scenarios where impermeable surfaces of parking lots are updated with porous materials (concrete grass tiling grid, green canopies, and trees), the rainwater flow is not calculated by ENVI-met. This missing factor would have had a stronger effect on the results as the average rain days in Vienna in August = 8.5 days.

Only trees' scenarios (TR) have changed the UTCI from strong heat stress level to moderate heat stress level. However, the average results of some streets at very low wind speed cannot be trusted because many UTCI is not calculated for the cells which have an air speed <0.5m/s. This could be an indication that it cannot be relied on UTCI as a thermal outdoor comfort indicator in all the cases.

The study concluded that the strategies which can have a strong impact on the surface temperatures of buildings and indoor temperatures (i.e., green facades), still can be inefficient in heat mitigation on the scale of an urban canyon. They could disadvantage the thermal comfort levels due to the high humidity caused by evapotranspiration.

The ENVI-met as a tool offers a very wide and detailed output. However, it lacks the water flow and thus the water content in a material (i.e., soil) does not differ and the emission levels don't change. Another point is the complicated user interface of ENVI-met and the complex process of data extraction for every climatic factor for every simulated hour. The data analysis has been conducted manually to select the grids representing the streets. That means that every single grid cell was selected and analyzed in a single step. The Grasshopper plugin had several bugs and instability but was helpful in generating different simulation scenarios in one step directly.

6 RECOMMENDATIONS FOR FUTURE RESEARCH

Future research should focus on a realistic approach regarding the strategies to be applied. This will depend on the ability of the studied area to encompass the recommended strategies. This depends on the factors of the dimensions of included urban canyons and the existing infrastructure in the underground level.

Regarding the aspect of simulations, a more comprehensive approach will require to take into consideration the aspect of rainfall events and water flow in the site model. Running simulations on several software tools would be a solution to overcome the limitations of every software tool as well as offering different evaluations for the impact of applied strategies.

Assessment of the thermal comfort in the urban fabric should be done using additional urban thermal comfort indices to the UTCI such as PET (Physiological equivalent temperature) or SET (Standard effective temperature), since UTCI cannot be calculated at air speed less than 0.5 m/s.

7 INDEX

7.1 List of abbreviations

(AE) 3
high albedo blocks in version A
(AE_A) 13
high albedo blocks in version B
(AE_B) 13
high albedo blocks in version C
(AE_C) 13
relative humidity
(RH) 1
trees
(TR) 3
trees in version A
(TR_A) 13
trees in version B
(TR_B) 13
trees in version C
(TR_C) 13
universal thermal climate index
(UTCI) 4
urban heat vulnerability index
(UHVI) 2
water vapour pressure
(vp) 9
wind velocity
(WV) 1

7.2 List of Figures

7.3 List of Tables

Table 1. Width of each urban canyon.....12
Table 2. Scenarios and their nomenclature.....13
Table 3. initial boundary conditions.....19
Table 4. Percentage of cells with version A where UTCI was not calculated in each street in green canopies' scenario (GC_A) and trees' scenario (TR_A) because UTCI cannot be calculated when air speed is < 0.5 m/s.....40
Table 5. Percentage of cells with version B where UTCI was not calculated in each street in green canopies' scenario (GC_B) and trees' scenario (TR_B) because UTCI cannot be calculated when air speed is < 0.5 m/s.....41

7.4 List of Equations

8 References

ADAPT-UHI. (2018). *Climate change adaptation scenarios for mödling*. https://eocs.blob.core.windows.net/adapt/ClimateChangeAdaptationandCostBenefitAnalysisforMoedling.pdf

Aleksandrowicz, O., Vuckovic, M., Kiesel, K., & Mahdavi, A. (2017). Current trends in urban heat island mitigation research: Observations based on a comprehensive research repository. *Urban Climate*, *21*, 1–26. https://doi.org/10.1016/j.uclim.2017.04.002

Ashrae. (2017). *Ashrae Sandard 55, Thermal environmental conditions for human occupancy*. https://www.techstreet.com/ashrae/standards/ashrae-55-2017?product_id=1994974#document&ashrae_auth_token=

Balany, F., Ng, A. W. M., Muttil, N., Muthukumaran, S., & Wong, M. S. (2020). Green infrastructure as an urban heat island mitigation strategy—a review. *Water*, *12*(12), 3577. https://doi.org/10.3390/w12123577

Błażejczyk, K., Broede, P., Fiala, D., Havenith, G., Holmér, I., Jendritzky, G., Kampmann, B [Bernhardt], & Kunert, A. (2010). Principles of the new universal thermal climate index (utci) and its application to bioclimatic research in European scale. *Miscellanea Geographica*, *14*(1), 91–102. https://doi.org/10.2478/mgrsd-2010-0009

Błażejczyk, K., Jendritzky, G., Bröde, P., Fiala, D., Havenith, G., Epstein, Y., Psikuta, A., & Kampmann, B [Bernhard] (2013). An introduction to the universal thermal climate index (utci). *Geographia Polonica*, *86*(1), 5–10. https://doi.org/10.7163/GPol.2013.1

Brandenburg, C., Damyanovic, D., Reinwald, F., Allex, B., Czachs, & Christina. (2018). *Urban Heat Island Strategy: City of Vienna.* Vienna Environmental Protection Department – Municipal Department 22. https://www.wien.gv.at/umweltschutz/raum/pdf/uhi-strategieplan-englisch.pdf

Climate Chip. (2021). *Utci street category*. http://www.climatechip.org/your-area-climate-data

Dec, E., Babiarz, B., & Sekret, R. (2018). Analysis of temperature, air humidity and wind conditions for the needs of outdoor thermal comfort. *E3S Web of Conferences*, *44*, 28. https://doi.org/10.1051/e3sconf/20184400028

Dimitrova, B., Vuckovic, M., Kiesel, K., & Mahdavi, A. (2014). Trees and the Microclimate of the Urban Canyon: A Case Study. http://dspace.epoka.edu.al/handle/1/953

Djedjig, R., Belarbi, R., & Bozonnet, E. (2017). Green wall impacts inside and outside buildings: Experimental study. *Energy Procedia*, *139*, 578–583. https://doi.org/10.1016/j.egypro.2017.11.256

ecoten. (2019). *Wiener hitzekarte*. https://www.wien.gv.at/stadtentwicklung/energie/hitzekarte.html

Farajzadeh, H., Saligheh, M., & Alijani, B. (2016). Application of Universal Thermal Climate Index in Iran from tourism perspective. *Journal of Natural Environmental Hazards*, *5*(7). https://doi.org/10.22111/jneh.2016.2658

Ferguson, B. K. (2005). *Porous pavements*. *Integrative studies in water management and land development*. Taylor & Francis. http://site.ebrary.com/lib/alltitles/docDetail.action?docID=10144006

Ferrari, A., Kubilay, A., Derome, D., & Carmeliet, J. (2020). The use of permeable and reflective pavements as a potential strategy for urban heat island mitigation. *Urban Climate*, *31*, 100534. https://doi.org/10.1016/j.uclim.2019.100534

Fröhlich, D., & Matzarakis, A. (Eds.) (2015). *Estimation of human-biometeorological conditions in south west Germany for the assessment of mitigation and adaptation potential*. https://www.researchgate.net/publication/281133508_Estimation_of_human-biometeorological_conditions_in_south_west_Germany_for_the_assessment_of_mitigation_and_adaptation_potential

Li, H., Harvey, J. T., Holland, T. J., & Kayhanian, M. (2013). The use of reflective and permeable pavements as a potential practice for heat island mitigation and stormwater management. *Environmental Research Letters*, *8*(1), 15023. https://doi.org/10.1088/1748-9326/8/1/015023

Lim, S. J., Vuckovic, M., Kiesel, K., & Mahdavi, A. (Eds.) (2014, May). *The variance of the urban microclimate in the city of Vienna, Austria*. : Vol. *259*. https://www.researchgate.net/publication/276209946_The_variance_of_the_urban_microclimate_in_the_city_of_Vienna_Austria

Marco Simoni. *Oia village-santorini, Greece.* Westend61. https://www.westend61.de/en/imageView/CUF43261/oia-village-santorini-greece

Matthias Winterer. (2019). *Kommt der wald in die stadt?* Wiener Zeitung. https://www.wienerzeitung.at/dossiers/wald/2019203-Kommt-der-Wald-in-die-Stadt.html?em_cnt_page=1

Nasrollahi, N., Ghosouri, A., Khodakarami, J., & Taleghani, M. (2020). Heat-mitigation strategies to improve pedestrian thermal comfort in urban

environments: A review. *Sustainability*, *12*(23), 10000. https://doi.org/10.3390/su122310000

Onishi, A., Cao, X., Ito, T., Shi, F., & Imura, H. (2010). Evaluating the potential for urban heat-island mitigation by greening parking lots. *Urban Forestry & Urban Greening*, *9*(4), 323–332. https://doi.org/10.1016/j.ufug.2010.06.002

Scholz, M., & Grabowiecki, P. (2007). Review of permeable pavement systems. *Building and Environment*, *42*(11), 3830–3836. https://doi.org/10.1016/j.buildenv.2006.11.016

Stadt Wien. (2021). *Stadt plan*. https://www.wien.gv.at/stadtplan/

Stadt Wien-MA 42. (2021). *Baumkataster*. https://www.wien.gv.at/umweltgut/public/

Storch, A., Schieder, W., Hollosi, B., Žuvela-Aloise, A., Prokop, G., Guggenberger, S., & See, L. (2020). *Urban Heat Island Hazard and Risk Indices for Austria.* https://doi.org/10.22022/esm/05-2020.86

Taleghani, M. (2018). Outdoor thermal comfort by different heat mitigation strategies- a review. *Renewable and Sustainable Energy Reviews*, *81*, 2011–2018. https://doi.org/10.1016/j.rser.2017.06.010

wikiwand. (2007). *Permeable paving*. https://www.wikiwand.com/en/Permeable_paving

Zentralanstalt für Meteorologie und Geodynamik. (2021). *Average rainfall days in August Vienna, Austria*. https://www.weather-atlas.com/en/austria/vienna-weather-august